Centre for Computational Finance and Economic Agents

WP061-12

Working Paper Series

Alexander Guarin, Xiaoquan Liu and Wing Lon Ng

Recovering Default Risk from CDS Spreads with a Nonlinear Filter

2012

CCFEA

www.ccfea.net

Recovering Default Risk from CDS Spreads with a Nonlinear Filter

Alexander Guarin*

Xiaoquan Liu†

Wing Lon Ng‡

28 March, 2012

Abstract

We propose a nonlinear filter to estimate the time-varying instantaneous default risk from the term structure of credit default swap (CDS) spreads. Based on the numerical solution of the Fokker-Planck equation (FPE) using a meshfree interpolation method, the filter performs a joint estimation of default intensities and CIR model parameters. As the FPE can account for nonlinear functions and non-Gaussian errors, the proposed framework provides more flexibility and accuracy. We test the nonlinear filter on simulated CDS spreads and apply it to daily CDS spreads of the Dow Jones Industrial Average component companies from 2005 to 2010 with supportive results.

Keywords: CDS Spreads, Meshfree Methods, Radial Basis Function Interpolation, Fokker-Planck Equation, CIR Model.

JEL Code: C11, C13, C63, C65, G12.

*Centre for Computational Finance and Economic Agents, University of Essex, Colchester, CO4 3SQ, UK and Banco de la República, Carrera 7 No. 14-78, Bogotá, Colombia. Email: aguarilo@banrep.gov.co.

†Corresponding author. Essex Finance Centre and Essex Business School, University of Essex, Colchester, CO4 3SQ, UK. Email: liux@essex.ac.uk. Phone: +44(0)1206 873849. Fax: +44(0)1206 873429.

‡Centre for Computational Finance and Economic Agents, University of Essex, Colchester, UK. Email: wlng@essex.ac.uk. Phone: +44(0)1206 874684.

1. Introduction

Accurately estimating the default risk of a certain firm is of major importance for many financial institutions and portfolio managers. In the recent finance literature, different approaches in pricing credit default swap (CDS) contracts have been proposed (see, for example, Houweling and Vorst (2005), Chen et al. (2008a), Chen et al. (2008b), Cao et al. (2010), and Ericsson et al. (2009)). However, these studies mainly focus on obtaining an accurate spread for the CDS contracts. In this paper, we are instead interested in evaluating the default probability and its time-varying dynamics from observed CDS spreads. We do so by developing a nonlinear filter that is able to jointly estimates the instantaneous default risk and the model parameters, including the volatility of default intensity, from the term structure of CDS spreads.

Credit default swap contracts are a popular credit derivative heavily traded in the financial market. They have gained considerable attention in the finance industry in recent years as they are able to hedge credit risk exposure and can be used to speculate. According to survey data from the Bank for International Settlements (BIS)[1], the total notional amount of the credit default swap market was $32 trillion in June 2011 while it was $6 trillion in 2004.

The rapid market growth is parallelled by the close scrutiny of these products in the literature to better understand and evaluate them as they provide crucial information on the dynamics of default probability not revealed by other financial instruments or market indicators. A detailed analysis of the credit risk implicit in CDS spreads becomes essential not only in their own pricing but also in the evaluation of more complex derivatives with a similar credit risk profile (Brigo and Mercurio (2006), and Liu et al. (2007)).

[1]Please see http://www.bis.org/statistics/derstats.htm for details.

There are two main approaches in the modeling of credit risk and the calibration of CDS spreads, namely structural models and reduced-form models. First, the structural models focus on the dynamics of firm's structural variables to determine the time of default (see, for example, Merton (1974), Pierides (1997), Giesecke (2006), Huang and Yu (2010), and Camâra et al. (2012)).

Secondly, the reduced-form models, which enjoy more empirical success, are a popular alternative in the literature. For example, Ueno and Baba (2006), Chen et al. (2008a), and Chen et al. (2008b) study corporate CDS contracts; Wang et al. (2009) use a copula approach for pricing credit default index swaps; while Zhang (2003), Carr and Wu (2007), Realdon (2007), and Pan and Singleton (2008) examine sovereign CDS securities. Chen et al. (2008a) provide an explicit solution for the valuation of CDS spreads when the interest rate and default intensity are correlated. Adopting the risk-neutral pricing framework, Pan and Singleton (2008) investigate the default risk and risk premium embedded in the term structure of sovereign CDS of Mexico, Turkey, and Korea. They suggest that the single-factor model in which the risk-neutral default risk follows a lognormal distribution is able to capture most of the variation in the CDS spreads and report economically significant risk premium.

In this paper, we adopt the reduced-form model approach due to its advantages in credit risk modeling compared with other methods (Houweling and Vorst (2005) and Löffler and Maurer (2011)). A common feature of this class of models is that default is assumed to be an exogenous random event that can occur at any time. Moreover, these methods are able to define a functional mapping from the default intensity and model parameters to the CDS spreads by using a pricing formula. However, neither the default intensity nor the parameter vector are observable in the market but need to be inferred.

Our paper addresses this issue as a filtering problem where the state of a stochastic dynamic system needs to be estimated from a sequence of noisy observations, which in essence are functions of latent state variables. Our model is hence related to Denault et al. (2009) and Carr and Wu (2010), who propose Kalman filters to estimate the model parameters and the default intensity. The Kalman filter is a conventional method often adopted for the estimation of state vectors in the presence of linear Gaussian systems. However, for most real-world applications, either the systems are nonlinear, or errors are non-Gaussian, or both.

In order to deal with these complications, researchers usually extend the Kalman filter using linear approximations or transformations of the initial problem (Raol et al. (2004), Daum (2005), and Grewal and Andrews (2008)). The extended Kalman filter is a suboptimal state estimator in nonlinear dynamic systems. It is based on the linearization of the state and/or measurement equations of the state-space model (Bar-Shalom et al. (2001)). The unscented Kalman filter arises as an alternative to the extended Kalman filter and uses a deterministic sampling approach. Under this scheme, the method employs a set of carefully chosen points to capture the mean and covariance of the Gaussian random variables (Wan and van Der Merwe (2001)) and in essence assumes that errors are Gaussian.

A more general and flexible approach in dealing with nonlinear or non-Gaussian filtering problem is based on the solution of the Fokker-Plank equation (FPE). This is a partial differential equation (PDE) that controls the dynamics of the conditional probability density function (PDF) of the state vector. This PDE has proven useful in the modeling of nonlinear and non-Gaussian problems as it does not assume perfect knowledge of the probability density (Challa and Bar-Shalom (2000), Kastella (2000), Daum

(2005), and Daum and Krichman (2006)). However, the FPE has closed-form solution only in very few cases and generally under restrictive assumptions. Hence, it needs to be approximated numerically. In this paper, we solve this approximation problem using the meshfree radial basis function (RBF) interpolation.

To the best of our knowledge, this is the first study that employs a nonlinear filtering method based on the FPE to evaluate the instantaneous default risk from credit derivatives. As the FPE is able to deal with models involving nonlinear functions and non-Guassian errors, it provides more flexibility in modeling and a higher level of accuracy in estimation when compared to the standard extended or unscented Kalman filter adopted in previous studies (eg. Denault, et al. (2009) and Carr and Wu (2010)). Hence, our paper contributes to the literature by developing a sophisticated nonlinear filter that is able to simultaneously infer the default risk and associated model parameters from the term structure of CDS spreads. This is especially useful and practical in the real world when variables need to be tracked in real time or a quick estimate of state variables is required (Kitagawa and Sato (2001), Liu and West (2001) and Wan and Nelson (2001)).

Our study is related to Driessen (2005) and Bakshi et al. (2006) who are also interested in estimating default risk but they use corporate bond data. Driessen (2005) adopts a maximum likelihood method with Kalman filter to infer risk premium associated with default jump risk from US corporate bond prices. Meanwhile, Bakshi et al. (2006) differentiate the roles of recovery rates and default probabilities in determining defaultable bond prices. Different from their methodology and data, we propose a nonlinear filter to perform a joint estimation of the latent default intensity and CIR parameters from CDS spreads. Our nonlinear filter is based on the recursive solution of the FPE by the RBF interpolation and updated via the Bayes' formula with each new observation.

We first evaluate the performance of the nonlinear filter in a numerical experiment. We assume realistic parameter values for the CIR (Cox et al. (1985)) model to generate CDS spreads. Next, we implement the nonlinear filter to recover default risk and parameter values from simulated spreads. Our numerical results show that the filter is able to infer the dynamics of the state vector and provides estimates for the default intensity and the model parameters with considerable levels of accuracy and reliability. This is very impressive given the range of values we assume for the parameters, including volatility between 8% and 20%.

In the subsequent empirical analysis, we use daily CDS spreads of the component companies of the Dow Jones Industrial Average (DJIA) from January 2005 to June 2010. Our sample precedes the onset of the banking crisis and covers the most turbulent episode of the US economy as a result of the crisis. The firms in our sample span different industries, some of which are more severely affected by the credit crunch than others. Hence the length and breadth of our sample data allow us to investigate both time series and cross sectional dynamics of corporate default risk before and during the financial crisis.

We find that the default intensities of individual firms were relatively stable and low before the mid-2007. Since then the instantaneous default risk kept increasing until the first quarter of 2009 and subsequently decreased but without dropping to the low level prior to the credit crunch. We also show that although the recent financial crisis affects all companies in our sample, there are important differences in the level of default risk experienced by firms in different sectors. In particular, the crisis has a more severe impact on the finance sector and the economy-sensitive sector of industrial goods, including American Express, the Bank of America, and the General Electric. In contrast, com-

panies in the sectors of consumer goods and health care experience much lower default intensities during the crisis period. Regarding the estimated model parameters, we observe structural changes after mid-2007 when there is a noticeable increase in the speed of mean reversion along with a rise in the volatility for default intensity. The estimated pricing errors as measured by root mean square error are low for the whole sample, but higher for companies with the highest default intensities.

The rest of the paper is organized as follows. In Section 2, we define the CDS spread and discuss technical aspects to compute the survival probability. Section 3 outlines the state-space model to estimate both the default intensity and the CIR parameters implicit in the CDS spreads. Section 4 introduces the nonlinear filter and its approximation by the RBF interpolation method. In Section 5, we first assess the performance of the nonlinear filter on simulated CDS spreads. This is followed by an empirical investigation and discussion using market CDS data. Finally, Section 6 concludes.

2. Credit Default Swap

In this section, we first review the definition of the CDS contract, its payoff and the formula to compute its fair spread (Section 2.1). We assume that both the short interest rate and the default intensity follow the one-factor CIR process (Section 2.2). This model, besides being a common choice in the literature, has an analytical solution. This feature is very convenient for our study because we are focused on the numerical solution of the FPE and the nonlinear filter rather than on the pricing method. Nonetheless, the filter can equally be applied to models with no closed-form solution (e.g. the exponential Vasicek model in Brigo and Mercurio (2006)). Finally, the expressions to compute zero-coupon bond prices and survival probabilities are presented (Section 2.3).

2.1 Definition and Payoff

A CDS is a contract between two entities, namely the protection buyer and the protection seller. Under this agreement, the CDS seller ensures protection to the buyer against a credit default event of a reference obligation issued by a third company.

We consider the CDS contract in the time $[0, T_b]$, $CDS_{0,b}$ and its expected payoff, $\Pi_{CDS_{0,b}}$. From protection seller's viewpoint, $\Pi_{CDS_{0,b}}$ is computed as the difference between the expected premium leg and the expected protection leg. The premium leg is the sum of two discounted factors. The first factor is the regular payments made by the protection buyer at times $T_1, \ldots, T_b$ until either the obligation reaches maturity at T_b without defaulting or it defaults at time $\tau \in (0, T_b)$. These fixed payments are denoted as the rate R (i.e. spreads) on the notional value of the contract. The second factor is the accrued amount between the last payment date $T_{\beta(\tau)-1}$ and the default time τ. Meanwhile, the protection leg consists of the contingent payment that a CDS seller makes to the buyer if the credit obligation defaults at time $\tau \in (0, T_b]$, otherwise this cash flow is 0.

Assume a stochastic interest rate r. The default time τ is modeled as the first jump of a Cox process with stochastic default intensity λ. Following Brigo and Alfonsi (2005), who show that the correlation between the interest rate and the default intensity has a negligible impact on CDS spreads, we assume that r and τ are independent.

Under these assumptions, Brigo and Mercurio (2006) show that the fair spread R can be written as

$$R = \frac{-L_{GD}\left[\int_0^{T_b} P(0,t)\, d_t \mathbb{Q}(\tau \geq t)\right]}{-\int_0^{T_b} P(0,t)\left(t - T_{\beta(t)-1}\right) d_t \mathbb{Q}(\tau \geq t) + \sum_{i=1}^{b} P(0,T_i)\,\alpha_i \mathbb{Q}(\tau \geq T_i)} \tag{1}$$

with

$$P(0,\cdot) = \mathbb{E}\left(\exp^{-\int_0^{\cdot} r_s ds}\right) \tag{2}$$

$$\mathbb{Q}(\tau \geq \cdot) = \mathbb{E}\left[\exp^{-\int_0^{\cdot} \lambda_s ds}\right], \tag{3}$$

where $P(0,\cdot)$ is the zero-coupon bond price at time 0 for maturity $(\cdot)$, $\mathbb{Q}(\tau \geq \cdot)$ is the probability at time 0 of surviving to a future time $(\cdot)$, L_{GD} is the loss given default on the underlying credit obligation, and α_i is the annualized time between T_{i-1} and T_i. Hence, we need to model the stochastic processes for the short interest rate and the default intensity.

2.2 The CIR Model

We assume that the short interest rate r_s follows the one-factor CIR model (see Cox et al. (1985)). Following Brigo and Mercurio (2006), for a suitable choice of the market price of risk, the factor r_s under the risk-neutral measure $\mathcal{Q}$ follows the process

$$dr_s = \kappa^r (\theta^r - r_s)\, ds + \sigma^r \sqrt{r_s} dW_s^r. \tag{4}$$

We also consider the same CIR process to model the default intensity λ_s. Under the same assumptions considered for r_s, the dynamics for λ_s under the risk-neutral measure $\mathcal{Q}$ is defined by

$$d\lambda_s = \kappa^\lambda \left(\theta^\lambda - \lambda_s\right) ds + \sigma^\lambda \sqrt{\lambda_s} dW_s^\lambda. \tag{5}$$

The parameters $\kappa^{(\cdot)}$, $\theta^{(\cdot)}$ and $\sigma^{(\cdot)}$ denote the speed of reversion, the long term mean level and the instantaneous volatility of the variable $(\cdot)$ under the CIR process. The variable $W_s^{(\cdot)}$ is a Wiener process for the variable $(\cdot)$.

2.3 Zero-coupon Bond Prices and the Survival Probability

Based on the CIR process described by equation (4), the zero-coupon bond price

$$P(r;0,t) = \mathbb{E}\left[\exp^{-\int_0^t r_s ds}\right] \tag{6}$$

is computed using the closed-form solution given by Brigo and Mercurio (2006, equations (3.24) and (3.25) on p. 66). The same analytical solution is performed to compute the survival probability

$$\mathbb{Q}(\lambda;\tau \geq t) = \mathbb{E}\left[\exp^{-\int_0^t \lambda_s ds}\right], \tag{7}$$

given the CIR process in equation (5).

3. State Vector and Parameter Estimation

This section discusses the joint estimation of the state and parameter vectors of a dynamic system using noisy observations. The problem is represented by a self-organizing model and its solution is given by the Bayesian approach (Section 3.1). This framework is used to describe the estimation procedure of both the short interest rate and the instantaneous default intensity (Section 3.2), along with their associated CIR parameter vectors from market data of interest rates and CDS spreads (Section 3.3).

3.1 The Self-organizing Model and the Bayesian Approach

Consider the filtering problem of recursively estimating the augmented state vector $\mathbf{x}_s$ from noisy observations of the vector $\boldsymbol{z}_s$, which are processed sequentially as they become available (see Kastella (2000) and Daum (2005)). The term s is the time index.

Following Challa and Bar-Shalom (2000), the self-organizing model of this dynamic system is given by

$$d\mathbf{x}_s = \mathbf{m}\left(\mathbf{x}_s\right) ds + \mathbf{G}\left(\mathbf{x}_s\right) d\mathbf{W}_s \tag{8}$$

$$\boldsymbol{z}_s = \mathbf{h}\left(\mathbf{x}_s, \boldsymbol{\epsilon}_s\right). \tag{9}$$

Equation (8) is an Ito process that describes the evolution of $\mathbf{x}_s$ over time. The state $\mathbf{x}_s$ and the drift $\mathbf{m}$ are n_1-dimensional column vectors, $\mathbf{G}$ is an $n_1 \times n_2$ diffusion matrix, and $\mathbf{W}_s$ is a n_2-dimensional Wiener process vector with covariance $\mathbf{Q}\left(s\right)$. Both $\mathbf{m}$ and $\mathbf{G}$ can be nonlinear.

Equation (9) is the measurement model. The function $\mathbf{h}$ relates the n_3-dimensional vector of noisy observations $\boldsymbol{z}_s$ to the augmented state vector $\mathbf{x}_s$ and the white noise vector $\boldsymbol{\epsilon}_s$. The function $\mathbf{h}$ can be nonlinear.

The vector $\mathbf{x}_s$ stacks the unobservable target state $\mathbf{y}_s$ and the unknown parameter vector $\boldsymbol{\psi}_s$ as

$$\mathbf{x}_s = \begin{bmatrix} \mathbf{y}_s \\ \\ \boldsymbol{\psi}_s \end{bmatrix}$$

such that $\boldsymbol{\psi}_s$ is automatically determined in the estimation of the state vector (see Kitagawa and Sato (2001)). Hence, equation (8) can be rewritten as

$$d\mathbf{y}_s = \mathbf{f}\left(\mathbf{y_s}\right) ds + \mathbf{G^y} d\mathbf{W_s^y} \tag{10}$$

$$d\boldsymbol{\psi}_s = \mathbf{G}^{\psi} d\mathbf{W}_s^{\psi}, \tag{11}$$

where $\mathbf{y}_s$ evolves according to the Ito equation (10) with drift function $\mathbf{f}$ and diffusion matrix $\mathbf{G}^y$. The parameters vector $\boldsymbol{\psi}$ is built as a vector of time-varying random variables

by adding small random perturbations (see Liu and West (2001)). Hence, equation (11) describes the vector $\boldsymbol{\psi}_s$ by a simple stochastic process with no drift and diffusion matrix $\mathbf{G}^{\psi}$. The variables $\mathbf{W}_s^y$ and $\mathbf{W}_s^{\psi}$ denote Wiener processes.

Following Ristic et al. (2004), from a Bayesian perspective the optimal estimate of the state $\mathbf{x}_s$ can be obtained from $p(\mathbf{x}_s \mid \mathsf{Z}_s)$, the posterior probability density function (PDF) of $\mathbf{x}_s$ given the observations up to time s, $\mathsf{Z}_s = [\boldsymbol{z}_1, \ldots, \boldsymbol{z}_s]$. Given an initial state $\mathbf{x}_0$ with PDF $p(\mathbf{x}_0)$, the posterior PDF can be recursively computed by a filter in two stages, namely prediction and update. The first stage gives the prior density of the state $p(\mathbf{x}_s \mid \mathsf{Z}_{s-1})$ using the probabilistic model of the dynamic system in equation (8) (see also Bar-Shalom et al. (2001) and Balaji (2009)). At the update stage, the prior density is adjusted with the new observation $\boldsymbol{z}_s$ in order to obtain the posterior PDF $p(\mathbf{x}_s \mid \mathsf{Z}_s)$ of the state $\mathbf{x}_s$ by the Bayes' rule

$$p(\mathbf{x}_s \mid \mathsf{Z}_s) = \frac{p(\boldsymbol{z}_s \mid \mathbf{x}_s)\, p(\mathbf{x}_s \mid \mathsf{Z}_{s-1})}{p(\boldsymbol{z}_s \mid \mathsf{Z}_{s-1})}, \tag{12}$$

where $p(\boldsymbol{z}_s \mid \mathbf{x}_s)$ is the likelihood function defined by both equation (9) and the statistics of $\boldsymbol{\epsilon}_s$, and

$$p(\boldsymbol{z}_s \mid \mathsf{Z}_{s-1}) = \int p(\boldsymbol{z}_s \mid \mathbf{x}_s)\, p(\mathbf{x}_s \mid \mathsf{Z}_{s-1})\, d\mathbf{x}_s$$

is a normalizing factor. Ristic et al. (2004) suggest that the optimal state $\mathbf{x}_s$ be estimated using either the minimum mean-square error (MMSE) estimator

$$\hat{\mathbf{x}}_{s|s} = E\{\mathbf{x}_s \mid \mathsf{Z}_s\} = \int \mathbf{x}_s \cdot p(\mathbf{x}_s \mid \mathsf{Z}_s)\, d\mathbf{x}_s \tag{13}$$

or the maximum a posteriori (MAP) estimator

$$\hat{\mathbf{x}}_{s|s} = \underset{\mathbf{x}_s}{argmax}\; p\left(\mathbf{x}_s \mid \mathsf{Z}_s\right). \tag{14}$$

3.2 Joint Interest Rate and CIR Parameter Estimation

We consider a filter that undertakes the recursive estimation of a joint vector formed by the hidden short interest rate r_s and the CIR model parameters at time s using noisy observations of the zero-coupon bond prices. The self-organizing model of this problem is given by

$$\begin{aligned}
\begin{bmatrix} dr_s \\ d\kappa_s^r \\ d\theta_s^r \\ d\sigma_s^r \end{bmatrix} &= \begin{bmatrix} \kappa_{s-1}^r\left(\theta_{s-1}^r - r_s\right)ds + \sigma_{s-1}^r\sqrt{r_s}dW_s^r \\ \vartheta_\kappa^r dW_{\kappa,s}^r \\ \vartheta_\theta^r dW_{\theta,s}^r \\ \vartheta_\sigma^r dW_{\sigma,s}^r \end{bmatrix} \\
\mathbf{P}_s &= \mathbf{h}^r\left(r_s, \boldsymbol{\psi}_s^r\right) + \boldsymbol{\epsilon}_s^r,
\end{aligned}$$

which can be written in a more compact form as follows,

$$\begin{bmatrix} dr_s \\ d\boldsymbol{\psi}_s^r \end{bmatrix} = \begin{bmatrix} \mathbf{f}^r\left(r_s, \boldsymbol{\psi}_{s-1}^r, W_s^r\right) \\ \boldsymbol{\vartheta}^r d\mathbf{W}_s^r \end{bmatrix} \tag{15}$$

$$\mathbf{P}_s = \mathbf{h}^r\left(r_s, \boldsymbol{\psi}_s^r\right) + \boldsymbol{\epsilon}_s^r. \tag{16}$$

Equation (15) is the system model of this problem. This equation describes the dynamics of both the time-dependent target state r_s and the unknown CIR parameter vector $\boldsymbol{\psi}_s^r = [\kappa_s^r, \theta_s^r, \sigma_s^r]$. The function $\mathbf{f}^r$ denotes the CIR stochastic process given in equation (4).

The dynamics of the vector $\boldsymbol{\psi}_s^r$ is modeled by a stochastic process with diffusion matrix $\boldsymbol{\vartheta}^r$. The term $\mathbf{W}_s^r$ denotes a Wiener process vector.

Equation (16) is the measurement model. The term $\mathbf{P}_s$ denotes a vector with zero-coupon bond prices for a set of maturities. The function $\mathbf{h}^r$ is given by the closed-form solution of equation (6). This solution defines zero-coupon bond prices in function of r_s and $\boldsymbol{\psi}_s^r$. The error $\boldsymbol{\epsilon}_s^r$ is a white noise with variance $\boldsymbol{\Sigma}^r$.

3.3 Joint Default Intensity and CIR Parameter Estimation

We consider a filtering model to estimate recursively a joint vector formed by the hidden default intensity λ_s and the unknown CIR process parameters using CDS spreads observed in the market. The augmented self-organizing model of this problem is defined by

$$\begin{bmatrix} d\lambda_s \\ d\kappa_s^\lambda \\ d\theta_s^\lambda \\ d\sigma_s^\lambda \end{bmatrix} = \begin{bmatrix} \kappa_{s-1}^\lambda \left(\theta_{s-1}^\lambda - \lambda_s\right) ds + \sigma_{s-1}^\lambda \sqrt{\lambda_s} dW_{\lambda,s} \\ \vartheta_\kappa^\lambda dW_{\kappa,s}^\lambda \\ \vartheta_\theta^\lambda dW_{\theta,s}^\lambda \\ \vartheta_\sigma^\lambda dW_{\sigma,s}^\lambda \end{bmatrix}$$

$$\mathbf{R}_s = \mathbf{h}^\lambda \left(\lambda_s, \boldsymbol{\psi}_s^\lambda\right) + \boldsymbol{\epsilon}_s^\lambda.$$

This model representation is summarized as

$$\begin{bmatrix} d\lambda_s \\ d\boldsymbol{\psi}_s^\lambda \end{bmatrix} = \begin{bmatrix} \mathbf{f}^\lambda \left(\lambda_s, \boldsymbol{\psi}_{s-1}^\lambda, W_s^\lambda\right) \\ \boldsymbol{\vartheta}^\lambda d\mathbf{W}_s^\lambda \end{bmatrix} \tag{17}$$

$$\mathbf{R}_s = \mathbf{h}^\lambda \left(\lambda_s, \boldsymbol{\psi}_s^\lambda\right) + \boldsymbol{\epsilon}_s^\lambda, \tag{18}$$

where the default intensity λ_s and the vector $\boldsymbol{\psi}_s^\lambda = \left[\kappa_s^\lambda, \theta_s^\lambda, \sigma_s^\lambda\right]$ are concatenated in order to form the system model in equation (17). The vector-valued function $\mathbf{f}^\lambda$ is given by the CIR process defined in equation (5). The evolution of vector $\boldsymbol{\psi}_s^\lambda$ is described by an Ito process with no drift and a diffusion matrix $\boldsymbol{\vartheta}^\lambda$. The vector $\mathbf{W}_s^\lambda$ is a Wiener process.

Equation (18) is the measurement equation of this problem. The term $\mathbf{R}_s$ denotes a vector at time s with CDS spreads for different maturities. The function $\mathbf{h}^\lambda$ corresponds to the CDS pricing formula given in equation (1). This equation depends on the values of the zero-coupon bond prices and the survival probabilities. The modeling of the interest rate r_s and zero-coupon bond prices is discussed in the previous subsection. Hence, these elements are assumed as given in the current filtering framework. The term $\boldsymbol{\epsilon}_s^\lambda$ represents a white noise error vector with variance $\boldsymbol{\Sigma}^\lambda$.

4. Nonlinear Filtering

The estimation of the joint default intensity and CIR model parameters implicit in the term structure of the CDS spreads is performed using a numerical nonlinear filter. This filter is based on the recursive solution of the Fokker-Planck equation (FPE) and the Bayes' formula. We first briefly introduce the nonlinear filter and provide a definition of the FPE (Section 4.1). We motivate the use of meshfree methods and in particular describe the radial basis function interpolation method (Section 4.2). Finally, we apply the method to approximate the solution of the FPE (Section 4.3).

4.1 The Numerical Filter

As discussed above, the optimal filtering estimator is obtained from the posterior PDF $p\left(\mathbf{x}_s \mid \mathsf{Z}_s\right)$. The estimator is recursively calculated by solving two related problems. The

first one computes the conditional density $p(\mathbf{x}_s \mid \mathsf{Z}_{s-1})$ from an initial PDF $p(\mathbf{x}_{s-1} \mid \mathsf{Z}_{s-1})$, while the second one updates $p(\mathbf{x}_s \mid \mathsf{Z}_{s-1})$ by the Bayes' formula to obtain the posterior PDF $p(\mathbf{x}_s \mid \mathsf{Z}_s)$.

Given an Ito stochastic equation to describe the dynamics of the target state $\mathbf{x}_s$, the PDF $p(\mathbf{x}_s \mid \mathsf{Z}_{s-1})$ can be computed as the solution of the FPE. This is a PDE that governs the time evolution of the conditional PDF of the state vector (Kushner and Dupuis (2001) and Balaji (2009)). Moreover, it is useful for modeling nonlinear functions and non-Gaussian errors (Daum (2005) and Daum and Krichman (2006)). Hence, the solution of the FPE and Bayes' formula provide a recursive method to obtain optimal estimates for the nonlinear filtering problem (Challa and Bar-Shalom (2000)).

Definition 1. The Fokker-Planck Equation (Challa and Bar-Shalom (2000)). Assume that the dynamics of the target state $\mathbf{x}_s$ is given by the stochastic differential equation (SDE)

$$d\mathbf{x}_s = \mathbf{m}(\mathbf{x}_s)\, ds + \mathbf{G}(\mathbf{x}_s)\, d\mathbf{W}_s$$

as defined in equation (8). Under the assumption that the prior density for the system above exists and is once continuously differentiable with respect to s and twice continuously differentiable with respect to $\mathbf{x}$, the evolution of the PDF of the state process $\tilde{p} = p(\mathbf{x}_s \mid \mathsf{Z}_{s-1})$ satisfies the FPE

$$\frac{\partial \tilde{p}}{\partial s} = -\sum_{i=1}^{n_1} \frac{\partial}{\partial x_i} \left[\mathbf{m}_i \tilde{p}\right] + \frac{1}{2} \sum_{i=1}^{n_1} \sum_{j=1}^{n_1} \frac{\partial^2}{\partial x_i \partial x_j} \left[\left(\mathbf{G}\mathbf{Q}\mathbf{G}'\right)_{i,j} \tilde{p}\right] \tag{19}$$

with initial condition given by $p(\mathbf{x}_{s-1} \mid \boldsymbol{Z}_{s-1})$.

In general, the FPE has to be approximated numerically due to the difficulty in obtaining an analytical solution. Grid-based standard methods have been employed for

solving this PDE. For example, Kastella (2000) and Challa and Bar-Shalom (2000) approximate the FPE with finite difference methods. Their results are used along with Bayes' formula to deal with optimal nonlinear filtering in real applications.

Nevertheless, the approximation of the FPE by standard fixed grid-based methods faces several difficulties. For instance, Daum (2005) and Daum and Krichman (2006) highlight that the computational complexity of these techniques grows exponentially with the dimension of the state vector, that their applications become very time-consuming in multi-dimensional problems, and that the grid does not change as the spatial domain evolves over time. Therefore, they suggest the meshfree methods as a novel alternative to mesh-based techniques for solving the FPE.

4.2 The Meshfree Methods and the Radial Basis Function Interpolation

The meshfree methods arise as novel numerical approximation techniques that overcome some weaknesses faced by the mesh-based methods such as the finite difference method (Duffy (2006)). These meshfree techniques have been used in applications of engineering that require an accurate, efficient and robust solution of problems associated with PDEs and the scattered data modeling (Fasshauer (2006, 2007)). Nonetheless, there are few studies that consider their application in finance (Mei and Cheng (2008) and Kelly (2009)).

Unlike the mesh-based approaches, the meshfree methods do not require the use of an underlying grid with connectivity among its knots. Instead, they are based on a set of independent nodes, which are scattered on the domain of the problem (Liu (2003) and Li and Liu (2004)). The meshfree methods are adaptive and versatile approximation techniques for the study of problems with complex geometries and irregular discretization

(Fasshauer (2007)). As there is no mesh, these methods are relatively easy to implement in multi-dimensional problems (Duffy (2006)).

One of the most popular meshfree methods is the radial basis function (RBF) interpolation, a powerful tool in scattered multivariate data modeling. They are widely used in engineering in providing numerical solutions to PDEs (see Liu (2003) and Fasshauer (2007)). In finance, the applications are concentrated in the solution of time-dependent PDEs for pricing options (Fasshauer et al. (2004), Pettersson et al. (2008) and Mei and Cheng (2008)) and credit derivatives (Guarin et al. (2011)).

The RBF interpolation deals with univariate basis functions and use a specific norm (commonly the Euclidean norm) to reduce a multi-dimensional problem into a one-dimensional one (Fasshauer (2006, 2007)). Hence, the approach deals with high-dimensional data with relative ease and its numerical results offer an efficient, highly accurate and versatile spatial approximation to the true solution (Duffy (2006)). In addition, the technique works easily with correlation terms without requiring special development (Fasshauer et al. (2004)). This feature is of crucial importance in the growing market of multi-asset derivative products.

Fasshauer (2006, 2007) explain that the RBF interpolation method approximates the value of a function as the weighted sum of RBFs. These functions are evaluated on a set of points called *centers*, which are quasi-randomly scattered over the domain of the problem. The weights are found by matching the approximated and observed values of the function. Once the interpolation weights are computed, they are used to estimate the value of the function at any point over the entire domain.

Following Fasshauer (2007), we consider the set of centers $\mathbf{Z} = [\mathbf{z}_1, \ldots, \mathbf{z}_K]'$ with $\mathbf{z}_k \in$

$\mathbb{R}^d$, $d \geq 1$ and the data values $g_k \in \mathbb{R}$. We assume that

$$g_k = f(\mathbf{z}_k, t), \quad k = 1, \ldots, K,$$

where f is an unknown function and t is the time. We also define $f(\mathbf{Z}, t)$ as a linear combination of K certain basic functions

$$f(\mathbf{Z}, t) \simeq \sum_{k=1}^{K} \delta_k(t) \varphi(\| \mathbf{Z} - \mathbf{z}_k \|), \quad k = 1, \ldots, K, \tag{20}$$

where the coefficients $\delta_k(t)$ are the unknown weights, $\varphi(\cdot)$ is the chosen RBF, and $\| \cdot \|$ is the Euclidean norm. Fasshauer (2007) shows that equation (20) is basically a system of linear equations

$$\begin{bmatrix} f(\mathbf{z}_1, t) \\ f(\mathbf{z}_2, t) \\ \vdots \\ f(\mathbf{z}_K, t) \end{bmatrix} \simeq \begin{bmatrix} \varphi(\| \mathbf{z}_1 - \mathbf{z}_1 \|) & \varphi(\| \mathbf{z}_1 - \mathbf{z}_2 \|) & \ldots & \varphi(\| \mathbf{z}_1 - \mathbf{z}_K \|) \\ \varphi(\| \mathbf{z}_2 - \mathbf{z}_1 \|) & \varphi(\| \mathbf{z}_2 - \mathbf{z}_2 \|) & \ldots & \varphi(\| \mathbf{z}_2 - \mathbf{z}_K \|) \\ \vdots & \vdots & \ddots & \vdots \\ \varphi(\| \mathbf{z}_K - \mathbf{z}_1 \|) & \varphi(\| \mathbf{z}_K - \mathbf{z}_2 \|) & \ldots & \varphi(\| \mathbf{z}_K - \mathbf{z}_K \|) \end{bmatrix} \begin{bmatrix} \delta_1(t) \\ \delta_2(t) \\ \vdots \\ \delta_K(t) \end{bmatrix}$$

which must be solved to obtain the interpolation coefficients $\delta_k(t)$. Once these weights are found, the value of the function f can be estimated at any set of points $\tilde{\mathbf{Z}} = [\tilde{\mathbf{z}}_1, \ldots, \tilde{\mathbf{z}}_L]'$ with $\tilde{\mathbf{z}}_l \in \mathbb{R}^d$ for $l = 1, \ldots, L$ and time t as

$$f\left(\tilde{\mathbf{Z}}, t\right) \simeq \sum_{k=1}^{K} \delta_k(t) \varphi\left(\| \tilde{\mathbf{Z}} - \mathbf{z}_k \|\right).$$

Table 1 lists four basic functions of RBFs often used in the literature. They are the Gaussian RBF, the MQ RBF, the cubic RBF, and the TPS RBF (Koc et al. (2003)).

4.3 Approximating the FPE-CIR Equation by the RBF Interpolation

In the following, we illustrate the application of the RBF interpolation to solve the FPE (19) of the system defined in equation (17). This model involves the dynamics of the default intensity λ_s and the CIR parameter vector $\boldsymbol{\psi}_s^{\lambda}$.

Given the one-factor CIR process in equation (5) for the variable λ_s, the FPE is written as

$$\frac{\partial \tilde{p}}{\partial s} = -\frac{\partial \left(\overline{\kappa}^{\lambda}\left(\overline{\theta}^{\lambda} - \lambda\right)\tilde{p}\right)}{\partial \lambda} + \frac{1}{2}\frac{\partial^2 \left(\left(\overline{\sigma}^{\lambda}\right)^2 \lambda \tilde{p}\right)}{\partial \lambda^2} + \frac{1}{2}\frac{\partial^2 \left(\left(\vartheta_{\kappa}^{\lambda}\right)^2 \tilde{p}\right)}{\partial \kappa^2} + \frac{1}{2}\frac{\partial^2 \left(\left(\vartheta_{\theta}^{\lambda}\right)^2 \tilde{p}\right)}{\partial \theta^2} + \frac{1}{2}\frac{\partial^2 \left(\left(\vartheta_{\sigma}^{\lambda}\right)^2 \tilde{p}\right)}{\partial \sigma^2} \tag{21}$$

with initial condition given by $p\left(\widehat{\boldsymbol{\lambda}}_{s-1} \mid \widehat{\mathsf{R}}_{s-1}\right)$.

The variable $\tilde{p} = p\left(\widehat{\boldsymbol{\lambda}}_s \mid \widehat{\mathsf{R}}_{s-1}\right)$ is the PDF of the state process, $\widehat{\boldsymbol{\lambda}}_s = \begin{bmatrix} \lambda_s \\ \boldsymbol{\psi}_s^{\lambda} \end{bmatrix}$ is the vector that stacks λ_s and $\boldsymbol{\psi}_s^{\lambda}$, and $\widehat{\mathsf{R}}_{s-1} = [\mathsf{R}_1, \ldots, \mathsf{R}_{s-1}]$ is the set of CDS spreads observed in the market up to time $s-1$. The term $\overline{(\cdot)}$ denotes the variable $(\cdot)$ at the time $s-1$, and therefore at time s that variable is a known constant.

After solving the derivatives in the PDE (21), we use the Crank-Nicolson averaging to approximate it in time such that

$$\begin{aligned}\frac{\tilde{p}_s - \tilde{p}_{s+1}}{\Delta s} + \left(\overline{\kappa}^{\lambda}\left(\overline{\theta}^{\lambda} - \lambda\right) - \left(\overline{\sigma}^{\lambda}\right)^2\right)\frac{\partial \tilde{p}_{s+\frac{1}{2}}}{\partial \lambda} - \frac{\left(\overline{\sigma}^{\lambda}\right)^2 \lambda}{2}\frac{\partial^2 \tilde{p}_{s+\frac{1}{2}}}{\partial \lambda^2} - \overline{\kappa}^{\lambda}\tilde{p}_{s+\frac{1}{2}} \\ - \frac{1}{2}\left(\left(\vartheta_{\kappa}^{\lambda}\right)^2 \frac{\partial^2 \tilde{p}_{s+\frac{1}{2}}}{\partial \kappa^2} + \left(\vartheta_{\theta}^{\lambda}\right)^2 \frac{\partial^2 \tilde{p}_{s+\frac{1}{2}}}{\partial \theta^2} + \left(\vartheta_{\sigma}^{\lambda}\right)^2 \frac{\partial^2 \tilde{p}_{s+\frac{1}{2}}}{\partial \sigma^2}\right) = 0,\end{aligned}$$

where $\tilde{p}_{s+\frac{1}{2}} = \frac{1}{2}\left(\tilde{p}_s + \tilde{p}_{s+1}\right)$. With this discretization and separating the elements in s and $s+1$ on both sides of the equation, we obtain

$$H_{+}^{\lambda}\tilde{p}_{s+1} = H_{-}^{\lambda}\tilde{p}_s, \tag{22}$$

where

$$H_{+}^{\lambda} = \left[1 - \frac{\Delta s}{2}\widetilde{H}^{\lambda}\right]$$
$$H_{-}^{\lambda} = \left[1 + \frac{\Delta s}{2}\widetilde{H}^{\lambda}\right] \tag{23}$$

and

$$\widetilde{H}^{\lambda} = \left(\overline{\kappa}^{\lambda}\left(\overline{\theta}^{\lambda} - \lambda\right) - \left(\overline{\sigma}^{\lambda}\right)^{2}\right)\frac{\partial}{\partial\lambda} - \frac{\left(\overline{\sigma}^{\lambda}\right)^{2}\lambda}{2}\frac{\partial^{2}}{\partial\lambda^{2}} - \overline{\kappa}^{\lambda} - \frac{1}{2}\left(\left(\vartheta_{\kappa}^{\lambda}\right)^{2}\frac{\partial^{2}}{\partial\kappa^{2}} + \left(\vartheta_{\theta}^{\lambda}\right)^{2}\frac{\partial^{2}}{\partial\theta^{2}} + \left(\vartheta_{\sigma}^{\lambda}\right)^{2}\frac{\partial^{2}}{\partial\sigma^{2}}\right).$$

Finally, we replace the variable $\tilde{p}$ in the last expression by the linear combination of RBFs to approximate in space. We obtain

$$\sum_{k=1}^{K}\delta_{k}^{\lambda}\left(s+1\right)H_{+}^{\lambda}\varphi\left(\widehat{\boldsymbol{\lambda}},\widehat{\boldsymbol{\lambda}}_{k}\right) = \sum_{k=1}^{K}\delta_{k}^{\lambda}\left(s\right)H_{-}^{\lambda}\varphi\left(\widehat{\boldsymbol{\lambda}},\widehat{\boldsymbol{\lambda}}_{k}\right), \tag{24}$$

where the coefficients $\delta_{k}^{\lambda}\left(s\right)$ for $k = 1, \ldots, K$ at time s are the weights, and $\varphi\left(\widehat{\boldsymbol{\lambda}},\widehat{\boldsymbol{\lambda}}_{k}\right)$ is the chosen RBF. To obtain the solution $\delta_{k}^{\lambda}\left(s+1\right)$, we have to iteratively solve the system of linear equations given the values $\delta_{k}^{\lambda}\left(s\right)$ from the previous step.

A similar solution is applied to estimate the vector $\widehat{\boldsymbol{r}}_{s} = \begin{bmatrix} r_{s} \\ \boldsymbol{\psi}_{s}^{r} \end{bmatrix}$ that stacks the short interest rate r_{s} and parameters $\boldsymbol{\psi}_{s}^{r}$. The variable r_{s} follows the CIR process in equation (4). The approximation of the FPE (19) of the system (15) by the RBF interpolation method is written as

$$\sum_{k=1}^{K}\delta_{k}^{r}\left(s+1\right)H_{+}^{r}\varphi\left(\widehat{\boldsymbol{r}},\widehat{\boldsymbol{r}}_{k}\right) = \sum_{k=1}^{K}\delta_{k}^{r}\left(s\right)H_{-}^{r}\varphi\left(\widehat{\boldsymbol{r}},\widehat{\boldsymbol{r}}_{k}\right), \tag{25}$$

where

$$H_+^r = \left[1 - \frac{\Delta s}{2}\widetilde{H}^r\right]$$
$$H_-^r = \left[1 + \frac{\Delta s}{2}\widetilde{H}^r\right] \tag{26}$$

and

$$\widetilde{H}^r = \left(\overline{\kappa}^r\left(\overline{\theta}^r - r\right) - \left(\overline{\sigma}^r\right)^2\right)\frac{\partial}{\partial r} - \frac{\left(\overline{\sigma}^r\right)^2 r}{2}\frac{\partial^2}{\partial r^2} - \overline{\kappa}^r - \frac{1}{2}\left(\left(\vartheta_\kappa^r\right)^2\frac{\partial^2}{\partial \kappa^2} + \left(\vartheta_\theta^r\right)^2\frac{\partial^2}{\partial \theta^2} + \left(\vartheta_\sigma^r\right)^2\frac{\partial^2}{\partial \sigma^2}\right).$$

5. Numerical Experiment and Empirical Analysis

In this section, we first evaluate the performance of the nonlinear filter to recover the default intensity λ_s and the CIR model parameters $\boldsymbol{\psi}_s^\lambda = \left[\kappa_s^\lambda, \theta_s^\lambda, \sigma_s^\lambda\right]$ from simulated CDS spreads (Section 5.1). The interest rate is assumed to be constant. We then introduce the empirical data in Section 5.2. The proposed filter is then performed on market data of zero-coupon bond prices and CDS spreads to estimate both r_s, λ_s and the associated CIR model parameters $\boldsymbol{\psi}_s^r$ and $\boldsymbol{\psi}_s^\lambda$, respectively (Section 5.3).

We employ the TPS-RBF stated in equation (31). This particular RBF is chosen for two reasons. First, it does not require the calibration of additional parameters as some RBFs do (e.g. the Gaussian- and MQ-RBF defined in equations (28) and (29), respectively). Second, a previous study in option pricing by Koc et al. (2003) shows the outstanding performance of the TPS-RBF compared with the Cubic-, Gaussian- and MQ-RBF.

The accuracy of the RBF method is assessed by the conventional measure, the root mean square error (RMSE) (see, for example, Fasshauer et al. (2004) and Fasshauer

(2007)). The RMSE is computed as

$$RMSE = \sqrt{\frac{1}{\mathcal{H}} \sum_{h=1}^{\mathcal{H}} \left(\hat{O}_h - O_h\right)^2}, \tag{27}$$

where $\mathcal{H}$ is the total number of observations.

5.1 The Numerical Experiment

We simulate a time series of 200 observations for the default intensity λ_s assuming that it follows the one-factor CIR process described by equation (5). Table 2 presents four sets of CIR model parameters employed in the simulation. Each set is used to simulate 50 observations. We consider that the initial default intensity is $\lambda_0 = 0.5\%$. This value has been reported for companies with historical credit rating of A (Chaplin (2005)). We also allow the volatility of default risk to reach 20% per annum, a very high level for the parameter.

Given the simulated values for the default intensity, we employ equation (1) to compute the vector of simulated CDS spreads. The simulation yields a 200×5 matrix $\mathbf{R}_s$ with CDS spreads for time $s = 1, \ldots, 200$ and maturities of 1, 3, 5, 7 and 10 years. A noise $\boldsymbol{\epsilon}_s^{\lambda}$ is added to $\mathbf{R}_s$. The process $\boldsymbol{\epsilon}_s^{\lambda}$ is drawn from a Normal distribution $\mathcal{N}\left(\mathbf{0}, \boldsymbol{\Sigma}^{\lambda}\right)$, where the variance matrix $\boldsymbol{\Sigma}^{\lambda} = 0.1\mathbf{I}$ and $\mathbf{I}$ is an identity matrix of dimension $d = 5$, the number of maturities. For simplicity, we consider a constant interest rate $r = 3\%$. We make conventional assumptions that the payments are quarterly, $\alpha = 0.25$, and the loss given default $L_{GD} = 60\%$ (Houweling and Vorst (2005) suggest that the model is comparatively less sensitive to the assumed recovery rate). As λ_s follows the CIR process, the survival probability $\mathbb{Q}\left(\mathbf{y}; \tau \geq t\right)$ is computed using the closed-form solution given by Brigo and Mercurio (2006, equations (3.24) and (3.25) on page 66).

Once the CDS spreads $\mathbf{R}_s$ have been simulated we assume that the vector $\mathbf{R}_s$ is the only available data we have. Our aim then is to recover the values of the default intensity λ_s and the CIR model parameters $\boldsymbol{\psi}_s^{\lambda} = \left[\kappa_s^{\lambda}, \theta_s^{\lambda}, \sigma_s^{\lambda}\right]$ using the self-organizing model described by equations (17) and (18).

At each time s, the vector $\mathbf{R}_s \in \mathbb{R}^5$ depends on the nonlinear function $\mathbf{h}^{\lambda}\left(\lambda_s, \boldsymbol{\psi}_s^{\lambda}\right)$ and the noise $\boldsymbol{\epsilon}_s^{\lambda}$. The function $\mathbf{h}$ is given by equation (1).

The dynamics of the default intensity $\lambda_s \in \mathbb{R}$ is characterized by equation (5). We assume that the parameters of the vector $\boldsymbol{\psi}_s^{\lambda} \in \mathbb{R}^3$ follow a random walk. Moreover, we consider for the parameter $(\cdot)$ a very small value for the variance, $\left(\vartheta_{(\cdot)}^{\lambda}\right)^2 = 1\mathrm{E}-3$, such that the parameter does not change too much over time (see Kitagawa and Sato (2001) and Liu and West (2001)).

The nonlinear filter is performed as follows. First, we approximate the FPE by the RBF interpolation to obtain an approximation of the conditional probability density $p\left(\widehat{\boldsymbol{\lambda}}_s \mid \widehat{\mathsf{R}}_{s-1}\right)$. To this end, we employ the iterative solution of the system (24). Once $p\left(\widehat{\boldsymbol{\lambda}}_s \mid \widehat{\mathsf{R}}_{s-1}\right)$ is computed, we apply the Bayes' rule given by equation (12) to sequentially obtain values for the probability $p\left(\widehat{\boldsymbol{\lambda}}_s \mid \widehat{\mathsf{R}}_s\right)$. Finally, we compute the optimal estimate of $\widehat{\boldsymbol{\lambda}}_s$ using the MMSE estimator defined by equation (13).

Figure 1 illustrates the result of the simulation and the performance of the nonlinear filter. In this experiment, the simulated values are considered as benchmark. In Panels A and C, the simulated values are plotted in black while the estimates are in blue. Panel A plots the simulated and estimated values of the default intensity λ_s. The estimated λ_s tracks the dynamics of the simulated values with high precision. The RMSE of the estimated λ_s is 1.4E-4. Panel B shows a comparison between the CIR parameters $\boldsymbol{\psi}_s^{\lambda} = \left[\kappa_s^{\lambda}, \theta_s^{\lambda}, \sigma_s^{\lambda}\right]$ used in the simulation and those inferred from the estimation. The figure

shows that the filter offers reliable estimates of the parameters even when the default risk is very volatile. Panel C plots the simulated and estimated values of CDS spreads while Panel D shows for each time s their RMSE. The average RMSE for the whole sample is 0.7204 basis points (bps) and the maximum value is 1.5529 bps. These results provide evidence of the accuracy of the estimation.

5.2 The CDS Data

The data for the empirical investigation consists of daily CDS spreads for 27 component companies of the Dow Jones Industrial Average (DJIA). Three component companies are left out because either the data do not cover the whole sample period or the CDS spreads are constant during long periods of time. We also obtain daily US Treasury constant maturity (TCM) bond rates as a proxy for the risk-free interest rate. The dataset includes observations for maturities of 1, 3, 5, 7 and 10 years. The sample period is from January 2005 to June 2010. All data are downloaded from the DataStream.

Table 3 summarizes the name of each company, its sector and the main statistics of the spreads for the 5-year CDS contracts. The time series exhibit some interesting patterns. First, there exist substantial cross-sectional differences across the firms; and second, there is a clear structural change in the levels of the default risk between two sub-periods before and after mid-2007, which we have arbitrarily chosen to divide our sample.

The first period, from January 2005 to June 2007, is characterized by low and stable CDS spreads. During this period, the term structure of CDS spreads has a downward trend. The highest average spreads are reported by telecommunications companies, including AT&T with 31.8 basis points (bps) and Verizon with 29.1 bps. AT&T and Verizon

also experience the highest maximum CDS spreads at 139.6 bps (20 January 2005) and 93.2 bps (18 October 2006), respectively, and the largest standard deviation. At the same time, the lowest values of CDS spreads are found in Johnson & Johnson, Exxon, Pfizer, 3M and Chevron, with average spreads of less than 11 bps. These companies belong to the sectors of health care, and oil & gas. During this period, the firms in the financial and industrial goods sectors, including the Bank of America and General Electric, enjoy relatively low average CDS spreads indicating a very small default risk.

In the second sub-period from July 2007 to June 2010, the dynamics and levels of the default risk change dramatically. The CDS spreads increase considerably with much higher volatility on average. The term structure is upward sloping until the first quarter in 2009, followed by a clear downward trend until the end of the year and then stabilizes. The highest average CDS rates are reported by Alcoa, General Electric, American Express and Bank of America with values of 274 bps, 247 bps, 193 bps and 128 bps, respectively. These companies, which belong to the worst affected sectors of basic materials, industrial goods, and financial services, also have standard deviations over 150 bps.

During the same period, the highest CDS maximum spreads were reached by General Electric and Alcoa with 1,037 bps (5 March 2009) and 1,156 bps (9 March 2009), respectively. These CDS spreads clearly reflects the pessimistic view from the market regarding the default risk of the two firms during the financial crisis. For example, on 3 March, 2009, the share price of General Electric fell below \$7 per share for the first time since May 1993. The conglomerate was later stripped of its AAA credit rating by Standard & Poor's on 12 March, 2009. The huge increase in CDS spreads captures these negative news in a timely manner.

5.3 Empirical Results and Discussion

The default intensity and the CIR model parameters are estimated using the nonlinear filter that we develop above. Contrary to the numerical experiment, in this empirical analysis the interest rate is no longer assumed to be constant. Therefore, it is necessary to infer r_s using the same nonlinear filter. Then the estimated short rates are used as inputs to compute the optimal default intensity and model parameters using the MMSE estimator defined in equation (13). In the following, we describe in turn the results for the short rate and the default intensity.

Estimated Short Interest Rate

In this subsection, we use the numerical nonlinear filter to estimate the augmented state vector of the self-organizing model described in equations (15) and (16). The estimation is carried out as described above, in particular Sections 3.1, 3.2, and 4.3.

Figure 2 presents the results of the joint estimation of r_s and $\boldsymbol{\psi}_s^r = [\kappa_s^r, \theta_s^r, \sigma_s^r]$. Panel A shows the US TCM rates. In Panel B, we plot the computed zero-coupon bond prices. Panel C presents the estimated short interest rate. This variable tracks closely the dynamics of the observed TCM plotted in Panel A. The short interest rate r_s goes up between 2005 and mid-2006, then it stabilizes around 4.5% until mid-2007. Afterward, it falls quickly to stabilize at very small values. Panel D shows the RMSE of the estimation, which takes as benchmark the zero-coupon bond prices at each time s. The RMSE is very small during the whole period. However, there is a clear increase in 2009 and 2010. For the first sub-period from January 2005 to June 2007, the average RMSE is 0.13%; in the second sub-period from July 2007 to June 2010, however, the average RMSE rises to 0.33%.

Finally, Panel E illustrates the time series of estimated parameters $[\kappa_s^r, \theta_s^r, \sigma_s^r]$. The long term mean level θ^r is quite stable and moves around the value 0.053 for the whole sample. The speed of reversion μ^r between the first and second period moved from 0.26 to 0.24 on average. For the same period, the volatility σ^r shows two clear levels. The instantaneous volatility is found to be around 0.12 on average for the first period, and drops slightly to 0.09 on average for the second subperiod.

These estimated values of the short interest rate r_0 and the CIR model parameters $[\kappa_s^r, \theta_s^r, \sigma_s^r]$ are now considered as given in order to carry out the estimation of the instantaneous default intensity λ_0 below.

Estimated Instantaneous Default Intensity

Similar to the previous subsection, we use the numerical filter to estimate the augmented state vector of the self-organizing model defined in equations (17) and (18). The estimation is undertaken as described in previous sections, in particular Sections 3.1, 3.3 and 4.3.

Figure 3 illustrates the time series of estimated default intensity for each company in our sample.[2] The companies are grouped by their respective sector. As we can see in this figure, before the mid-2007 the default intensity for all companies is relatively stable and very low with an average of about 0.012%. However, since the second half of 2007, the default intensity has experienced considerable changes in its dynamics. First, the default intensity increases dramatically between July 2007 and the first quarter of 2009 when it tends to reach its maximum value for most companies in our sample. Note that March 2009 was a particularly bad month for the US economy with a negative report on unemployment figures and with the Dow Jones and S&P 500 indexes both hitting a

[2]Please note that there are different scales on the Y-axis for some plots.

12-year low on the 9th of the month. Afterwards the default intensity gradually decreases but without dropping to the low levels seen before the banking crisis.

Table 4 summarizes the main statistics of the estimated default intensities. Although during the financial crisis, the default risk experiences similar dynamics for all companies, there are important differences in the levels reached by different firms and sectors.

The highest default intensities are reached by Alcoa in the sector of basic materials and General Electric in the sector of industrial goods, with values of 20% (9 March 2009) and 19.4% (5 March 2009), respectively. The aluminum producer Alcoa is an economy-sensitive company. Its stock price dropped to a historic low on 2 March 2009 as the US economy struggled to deal with the turmoil of the credit crunch. At the same time, General Electric also faced huge challenges due to the banking crisis. The fact that their instantaneous default intensity peaked at this time not only substantiates the efficiency of the CDS market as a place for trading company specific information and expectation but also attests to the accuracy and reliability of our nonlinear filter to recover such information from market CDS spreads.

Not surprisingly, other firms with very high levels of default intensity are in the financial sector. For example, the American Express is shown to have experienced a maximum default intensity of 15.3% while the Bank of America reaches a value of 11.1%. These firms are followed by Caterpillar, J.P. Morgan, Boeing and Home Depot with maximum probabilities of 7.17%, 5.16%, 4.33% and 4.16%, respectively.

In contrast, companies in the sectors of health care, oil & gas, soft drinks and consumer services have a smoother ride during the credit crunch. The low levels of instantaneous default intensities are inferred for companies such as Johnson & Johnson, Exxon, and Coca Cola between 0.78% and 0.89%. These firms are followed by McDonalds, 3M and

United Technologies with default intensities between 1.06% and 1.27%.

In summary, our results show that the banking crisis affects all companies in our sample. However, the crisis has inflicted more distress on firms in the financial services and industrial sectors in terms of skyrocketed default risk. Meanwhile, our method is able to accurately recover the dynamics of the default intensities for individual firms over time and suggest a clear differentiation between firms in different sectors.

Tables 5 and 6 report the estimated CIR model parameters and the RMSE of the estimation for the sub-period from 2005 to mid-2007 and from mid-2007 to 2010, respectively. These values are computed as average of their estimated parameters over the two sub-periods. The results show a large increase in the average speed of reversion and instantaneous volatility. The average speed of reversion goes up from 0.068 to 0.228 and the volatility of the default risk almost doubles from 0.041 before the banking crisis to 0.081. Again this is also consistent with the unfolding of the state of the economy during that turbulent period. In addition, the computed RMSE of the estimation is 1.57 bps on average during the first period, and rises to 3.39 bps in the second period. The companies with the highest estimated errors include Alcoa, General Electric, Home Depot, Bank of America, American Express and J.P. Morgan, the same firms with high default intensities.

6. Conclusion

Credit default risk is of major concern to financial markets and risk managers, providing them with information on the probability of a company's potential financial distress, bankruptcy or liquidation. Various approaches have been proposed in the literature to evaluate CDS products, but not all of them concentrates on the actual default probability

and its time-varying dynamics.

To fill this important gap, we develop a nonlinear filter to jointly estimate the latent default intensity and unknown CIR parameter vector implicit in the term structure of CDS spreads. The filter is estimated on the basis on the recursive solution of the Fokker-Planck equation (FPE) by the radial basis function (RBF) interpolation and updated via the Bayes' formula with each new observation. As the FPE is able to deal with models involving nonlinear functions and non-Gaussian errors, it is more flexible compared to the standard extended or unscented Kalman filters widely adopted in the literature. In addition, the filter allows for the simultaneous estimation of state variables and model parameters, it is hence of great help to practitioners.

In order to evaluate the performance of the filter, we first undertake a numerical experiment using simulated CDS spreads. The results show that the filter provides reliable and accurate estimates of the model parameters and the estimated dynamics of the default risk closely tracks the simulated process.

We apply the nonlinear filter to 27 component companies of the DJIA using daily CDS spreads with five different maturities between January 2005 to June 2010. Our empirical results suggest that the banking crisis has triggered a big increase in the default risk of all sample firms and led to a structural change in model parameters. However, the level of default risk reached by different entities and sectors show important differences. In particular, the credit crunch has a dramatic effect on the financial firms such as the American Express and the Bank of America compared with firms in the health care and consumer services. In addition, the time series variation in the default risk we obtain for these firms is consistent with the unfolding of market events during the banking crisis, a testimony of the accuracy and efficiency of our numerical filter.

References

Bakshi, G., Madan, D., Zhang, F., 2006. Understanding the role of recovering in default risk models: Empirical comparisons and implied recovery rates. Working paper, University of Maryland.

Balaji, B., 2009. Continuous-discrete path integral filtering. Entropy 11, 402–430.

Bar-Shalom, Y., Li, X., Kirubarajan, T., 2001. Estimation with Applications to Tracking and Navigation: Theory, Algorithms, and Software. John Wiley & Sons, New York.

Brigo, D., Alfonsi, A., 2005. Credit default swap calibration and derivatives pricing with the SSRD stochastic intensity model. Finance and Stochastics 9, 29–42.

Brigo, D., Mercurio, F., 2006. Interest Rate Models: Theory and Practice with Smile, Inflation and Credit. Springer, Berlin.

Camâra, A., Popova, I., Simkins, B., 2012. A comparative study of the probability of default for global financial firms. Journal of Banking and Finance 36, 717–732.

Cao, C., Yu, F., Zhong, Z., 2010. The information content of option-implied volatility for credit default swap valuation. Journal of Financial Markets 13, 321–343.

Carr, P., Wu, L., 2007. Theory and evidence on the dynamic interactions between sovereign credit default swaps and currency options. Journal of Banking and Finance 31, 2383–2403.

Carr, P., Wu, L., 2010. Stock options and credit default swaps: A joint framework for valuation and estimation. Journal of Financial Econometrics 8, 409–449.

Challa, S., Bar-Shalom, Y., 2000. Nonlinear filter design using Fokker-Planck-Kolmogorov probability density evolutions. IEEE Transactions on Aerospace and Electronic Systems 36, 309–315.

Chaplin, G., 2005. Credit Derivatives, Risk Management, Trading and Investing. John Wiley & Sons, Chichester.

Chen, R., Cheng, X., Fabozzi, F., Liu, B., 2008a. An explicit, multi-factor credit default swap pricing model with correlated factors. Journal of Financial and Quantitative Analysis 43, 123–160.

Chen, R., Cheng, X., Liu, B., 2008b. Estimation and evaluation of the term structure of credit default swaps: An empirical study. Insurance: Mathematics and Economics 43, 339–349.

Cox, J., Ingersoll, J., Ross, S., 1985. A theory of the term structure of interest rates. Econometrica 53, 385–407.

Daum, F., 2005. Nonlinear filters: Beyond the Kalman filter. Aerospace and Electronic Systems Magazine, IEEE 20, 57–69.

Daum, F., Krichman, M., 2006. Meshfree adjoint methods for nonlinear filtering. In: Aerospace Conference, 2006. IEEE, Big Sky, MT, pp. 1–16.

Denault, M., Gauthier, G., Simonato, J.-G., 2009. Estimation of physical intensity models for default risk. Journal of Futures Markets 29, 95–113.

Driessen, J., 2005. Is default event risk priced in corporate bonds. Review of Financial Studies 18, 165–195.

Duffy, D., 2006. Finite Difference Methods in Financial Engineering: A Partial Differential Equation Approach. John Wiley & Sons, Chichester.

Ericsson, J., Jacobs, K., Oviedo, R., 2009. The determinants of credit default swap premia. Journal of Financial and Quantitative Analysis 44, 109–132.

Fasshauer, G., 2006. Meshfree methods. In: Rieth, M., Schommers, W. (Eds.), Handbook of Theoretical and Computational Nanotechnology. Vol. 10. American Scientific Publishers, pp. 33–97.

Fasshauer, G., 2007. Meshfree Approximation Methods with MATLAB. World Scientific Publishers, Singapore.

Fasshauer, G., Khaliq, A., Voss, D., 2004. Using meshfree approximation for multi-asset American options. Journal of Chinese Institute of Engineers 27, 563–571.

Giesecke, K., 2006. Default and information. Journal of Economic Dynamics and Control 30, 2281–2303.

Grewal, M., Andrews, A., 2008. Kalman Filtering: Theory and Practice Using MATLAB. John Wiley & Sons, New Jersey.

Guarin, A., Liu, X., Ng, W. L., 2011. Enhancing credit default swap valuation with meshfree methods. European Journal of Operational Research 214, 805–813.

Houweling, P., Vorst, T., 2005. Pricing default swaps: Empirical evidence. Journal of International Money and Finance 24, 1200–1225.

Huang, S. J., Yu, J., 2010. Bayesian analysis of structural credit risk models with microstructure noises. Journal of Economic Dynamics and Control 34, 2259–2272.

Kastella, K., 2000. Finite difference methods for nonlinear filtering and automatic target recognition. In: Bar-Shalom, Y., Dale Blair, W. (Eds.), Multitarget-Multisensor Tracking: Applications and Advances. Vol. 3. Artech House Publishers, London, pp. 233–258.

Kelly, M., 2009. Evaluation of financial options using radial basis functions in mathematica. Mathematica Journal 11, 333–357.

Kitagawa, G., Sato, S., 2001. Monte Carlo smoothing and self-organising state-space model. In: Doucet, A., De Freitas, N., Gordon, N. (Eds.), Sequential Monte Carlo Methods in Practice. Springer, New York, pp. 177–196.

Koc, M., Boztosun, I., Boztosun, D., 2003. On the numerical solution of Black-Scholes equation. In: International Workshop on Meshfree Methods. Instituto Superior Técnico - ICIST, Lisbon, Portugal, pp. 1–6.

Kushner, H., Dupuis, P., 2001. Numerical Methods for Stochastic Control Problems in Continuous Time. Springer, New York.

Li, S., Liu, W., 2004. Meshfree Particle Methods. Springer, Berlin.

Liu, B., Kocagil, A., Gupton, G., 2007. Fitch equity implied rating and probability of default model. Quantitative Research Special Report, Fitch Solutions.

Liu, G., 2003. Mesh Free Methods: Moving Beyond the Finite Element Method. CRC Press, London.

Liu, J., West, M., 2001. Combined parameter and state estimation in simulation-based filtering. In: Doucet, A., De Freitas, N., Gordon, N. (Eds.), Sequential Monte Carlo Methods in Practice. Springer, New York, pp. 197–223.

Löffler, G., Maurer, A., 2011. Incorporating the dynamics of leverage into default prediction. Journal of Banking and Finance 35, 3351–3361.

Mei, L., Cheng, P., 2008. Multivariable option pricing using quasi-interpolation based on radial basis functions. In: 4th International Conference on Intelligent Computing. SPIE, Shanghai, China, pp. 620–627.

Merton, R., 1974. On the pricing of corporate debt: The risk structure of interest rate. Journal of Finance 29, 449–470.

Pan, J., Singleton, K., 2008. Default and recovery implicit in the term structure of sovereign CDS spreads. Journal of Finance 63, 2345–2384.

Pettersson, U., Larsson, E., Marcusson, G., Persson, J., 2008. Improved radial basis function methods for multi-dimensional option pricing. Journal of Computational and Applied Mathematics 222, 82–93.

Pierides, Y. A., 1997. The pricing of credit risk derivatives. Journal of Economic Dynamics and Control 21, 1579–1611.

Raol, J., Girija, G., Singh, J., 2004. Modelling and Parameter Estimation of Dynamic Systems. The Institution of Electrical Engineers, London.

Realdon, M., 2007. A two-factor Black-Karasinski sovereign credit default swap pricing model. ICFAI Journal of Derivatives Markets 4, 6–21.

Ristic, B., Arulampalam, S., Gordon, N., 2004. Beyond the Kalman Filter. Particle Filters for Tracking Applications. Artech House Publishers, London.

Ueno, Y., Baba, N., 2006. Default intensity and expected recovery of Japanese banks and

the government: New evidence from the CDS market. Working Paper 6-E-04, Bank of Japan.

Wan, E., Nelson, A., 2001. Dual extended Kalman filter methods. In: Haykin, S. (Ed.), Kalman Filtering and Neural Networks. John Wiley & Sons, New York, pp. 175–220.

Wan, E. A., van Der Merwe, R., 2001. The unscented kalman filter. In: Haykin, S. (Ed.), Kalman Filtering and Neutral Networks. John Wiley & Sons, New York, pp. 221–280.

Wang, D., Rachev, S. T., Fabozzi, F. J., 2009. Pricing of credit default index swap tranches with one-factor heavy-tailed copula models. Journal of Empirical Finance 16, 201–215.

Zhang, F., 2003. What did the credit market expect of Argentina default? Evidence from default swap data. Working Paper FEDS 2003-25, The Federal Reserve Board.

Table 1. Examples of popular radial basis functions (RBFs)

Gaussian RBF: $\varphi(c_k) = \exp^{-\varepsilon^2 c_k^2}$	(28)
MQ-RBF: $\varphi(c_k) = \sqrt{\varepsilon^2 + c_k^2}$	(29)
Cubic RBF: $\varphi(c_k) = c_k^3$	(30)
TPS-RBF: $\varphi(c_k) = c_k^4 \ln(c_k)$	(31)

In this table, $\varphi(c_k)$ is the basic function of the RBF $\mathbf{\Phi}_k$ centered on c_k, defined as $c_k = \| \mathbf{Z} - \mathbf{z}_k \|$, where $\| \cdot \|$ is the Euclidean norm, $\mathbf{Z}$ is the set of centers $[\mathbf{z}_1, \ldots, \mathbf{z}_K]'$, and $\mathbf{z}_k \in \mathbb{R}^d$ is the k-th center. The constant ε is a shape parameter.

Table 2. Simulation Parameters of the Default Intensity

Observation	κ^λ	θ^λ	σ^λ
1 - 50	0.23	0.030	0.08
51 - 100	0.30	0.055	0.12
101 - 150	0.37	0.065	0.15
151 - 200	0.46	0.076	0.20

This table reports four sets of parameters used in the simulation of the default intensity for samples of 50 observations. Each set consists of the parameters κ^λ, θ^λ and σ^λ for the one-factor CIR model. The experiment is performed to simulate a total of 200 observations.

Table 3. Summary statistics of 5-year CDS spreads

Company Name	Industry	January 2005 - June 2007						July 2007 - June 2010					
		Mean	Std.	Skew	Kurt	Min	Max	Mean	Std.	Skew	Kurt	Min	Max
3M Co.	Industrials	7.2	1.6	0.9	3.8	4.3	13.5	46.3	28.1	1.4	4.7	11.5	140.0
Alcoa Inc.	Basic Materials	24.7	7.7	1.3	4.4	14.0	53.0	274.4	234.8	1.3	3.8	28.9	1156.3
American Express Co.	Financials	19.0	6.0	0.2	2.4	8.0	34.3	193.1	150.3	1.5	4.7	17.0	712.0
AT&T Inc.	Telecommunications	31.8	21.2	2.3	11.5	7.5	139.6	45.1	20.5	1.1	4.0	12.2	118.0
Bank of America Corp.	Financials	13.6	3.8	0.4	2.4	7.8	23.8	127.8	68.7	1.1	4.8	13.5	400.7
Boeing Co.	Industrials	15.3	5.1	0.5	2.6	6.5	30.5	90.9	62.1	1.1	3.5	12.4	295.0
Caterpillar Inc.	Industrials	18.1	4.4	1.3	5.7	11.2	39.7	100.6	81.0	1.5	4.5	16.2	427.5
Chevron Corp.	Oil & Gas	10.3	3.8	0.0	1.6	3.4	16.5	46.4	27.8	1.1	3.9	9.9	135.6
Coca-Cola Co.	Consumer Goods	10.4	2.3	0.2	2.0	6.4	15.5	43.4	19.1	0.7	3.1	12.0	104.7
E.I. DuPont de Nemours & Co.	Basic Materials	17.3	4.3	0.2	2.0	8.5	27.0	66.1	38.5	1.2	4.2	16.7	230.5
Exxon Mobil Corp.	Oil & Gas	6.1	2.4	0.2	1.6	2.5	11.5	33.7	22.7	1.7	6.0	6.0	115.0
General Electric Co.	Industrials	17.8	5.2	0.5	2.3	11.0	30.5	246.8	198.3	1.2	3.9	17.3	1037.2
Hewlett-Packard Co.	Technology	21.6	9.9	0.8	3.9	7.4	62.5	45.5	21.1	1.3	4.8	15.0	136.7
Home Depot Inc.	Consumer Services	14.1	4.7	0.9	3.0	7.3	30.8	121.1	71.4	1.1	3.7	28.5	360.0
International Business Machines Corp.	Technology	15.9	5.3	0.1	2.5	5.2	30.0	48.7	23.7	1.2	4.5	15.0	143.3
Johnson & Johnson	Health Care	5.0	1.9	0.8	2.6	2.9	10.5	33.7	17.8	0.4	2.5	7.0	80.3
JPMorgan Chase & Co.	Financials	20.9	6.3	0.9	3.2	11.0	43.5	91.1	40.6	0.8	3.3	19.8	242.1
Kraft Foods Inc. Cl A	Consumer Goods	23.5	5.3	0.0	2.4	12.0	36.1	74.2	26.1	0.1	2.6	23.5	169.3
McDonald's Corp.	Consumer Services	20.1	8.5	0.7	2.1	8.5	39.2	37.4	13.0	0.5	2.3	15.9	79.9
Merck & Co. Inc.	Health Care	16.9	9.5	0.8	2.6	5.5	40.5	38.1	17.5	0.5	2.7	10.5	90.0
Pfizer Inc.	Health Care	7.2	3.6	1.4	4.9	3.0	20.0	48.0	26.8	0.8	3.9	7.0	132.0
Procter & Gamble Co.	Consumer Goods	13.4	3.9	-0.3	1.9	5.4	20.5	57.8	33.6	1.2	3.4	11.2	157.8
Travelers Cos. Inc.	Financials	27.8	8.0	0.1	2.3	14.5	57.5	75.9	29.2	0.3	2.5	21.5	158.3
United Technologies Corp.	Industrials	14.9	3.9	1.4	5.8	8.5	33.2	54.8	29.3	1.4	4.4	16.2	154.0
Verizon Communications Inc.	Telecommunications	29.1	19.3	1.9	5.1	14.8	93.2	74.1	35.7	0.6	3.0	17.5	180.0
Wal-Mart Stores Inc.	Consumer Services	10.5	3.5	0.5	2.5	4.9	21.2	51.3	26.2	1.1	3.2	10.0	130.0
Walt Disney Co.	Consumer Services	23.8	10.5	0.4	2.1	7.7	49.2	51.2	21.3	1.1	4.6	14.4	135.0

This table summarizes the main statistics of 5-year CDS spreads of 27 component companies of the DJIA between January 2005 and June 2010. The companies are classified by industry. The analysis considers the following statistics: mean, standard deviation, skewness, kurtosis, minimum and maximum. The sample period is divided in two subperiods, namely from January 2005 to June 2007 and from July 2007 to June 2010. The values are reported in basis points.

Table 4. Summary statistics for the estimated default intensity

Company Name	January 2005 - June 2007			July 2007 - June 2010		
	Mean	**Std.**	**Max**	**Mean**	**Std.**	**Max**
3M Co.	0.002	0.001	0.008	0.30	0.31	1.24
Alcoa Inc.	0.006	0.015	0.176	3.38	4.42	20.00
American Express Co.	0.005	0.005	0.040	3.68	3.78	15.33
AT&T Inc.	0.011	0.028	0.158	0.31	0.33	1.49
Bank of America Corp.	0.014	0.010	0.061	1.88	2.05	11.12
Boeing Co.	0.003	0.004	0.041	0.74	0.69	4.33
Caterpillar Inc.	0.004	0.008	0.163	1.06	1.45	7.17
Chevron Corp.	0.023	0.012	0.084	0.35	0.31	1.36
Coca-Cola Co.	0.017	0.011	0.053	0.28	0.17	0.89
E.I. DuPont & Co.	0.012	0.011	0.082	0.46	0.55	2.44
Exxon Mobil Corp.	0.009	0.007	0.053	0.21	0.21	0.78
General Electric Co.	0.026	0.017	0.074	4.16	4.53	19.35
Hewlett-Packard Co.	0.010	0.009	0.129	0.38	0.40	1.99
Home Depot Inc.	0.005	0.009	0.126	1.18	1.11	4.16
IBM Corp.	0.010	0.007	0.077	0.36	0.45	2.43
Johnson & Johnson	0.005	0.003	0.024	0.29	0.20	0.81
JPMorgan Chase & Co.	0.025	0.017	0.093	1.06	0.93	5.16
Kraft Foods Inc. Cl A	0.033	0.034	0.181	0.56	0.39	1.58
McDonald's Corp.	0.012	0.021	0.144	0.24	0.25	1.06
Merck & Co. Inc.	0.010	0.010	0.066	0.32	0.31	1.81
Pfizer Inc.	0.006	0.003	0.030	0.33	0.39	1.71
Procter & Gamble Co.	0.009	0.006	0.038	0.41	0.43	1.56
Travelers Cos. Inc.	0.031	0.024	0.201	0.69	0.59	2.00
United Technologies	0.004	0.004	0.036	0.40	0.30	1.27
Verizon Communications	0.006	0.010	0.137	0.49	0.48	1.84
Wal-Mart Stores Inc.	0.017	0.014	0.145	0.51	0.43	1.75
Walt Disney Co.	0.003	0.002	0.021	0.33	0.36	1.53
Average	0.012	0.011	0.090	0.902	0.956	4.302

This table provides summary statistics of the estimated default intensity λ of 27 component companies of the DJIA. The instantaneous default intensity λ_0 is inferred from CDS spreads with maturities of $t = 1, 3, 5, 7$ and 10 years. The two subperiods considered are from January 2005 to June 2007 and from July 2007 to June 2010. The statistics reported include the mean, the standard deviation and the maximum. The values are reported in percentages.

Table 5. Estimated CIR parameters: CDS spreads, January 2005-June 2007

Company Name	**January 2005 - June 2007**			
	κ^{λ}	μ^{λ}	σ^{λ}	**RMSE (bps)**
3M Co.	0.090 (0.009)	0.006 (0.001)	0.028 (0.003)	1.556 (0.951)
Alcoa Inc.	0.084 (0.008)	0.023 (0.006)	0.041 (0.005)	2.347 (1.205)
American Express Co.	0.118 (0.034)	0.012 (0.003)	0.051 (0.010)	0.912 (0.557)
AT&T Inc.	0.047 (0.018)	0.048 (0.009)	0.021 (0.006)	3.587 (0.782)
Bank of America Corp.	0.122 (0.013)	0.009 (0.002)	0.042 (0.005)	1.044 (0.420)
Boeing Co.	0.047 (0.019)	0.024 (0.002)	0.044 (0.008)	1.377 (0.557)
Caterpillar Inc.	0.070 (0.040)	0.022 (0.005)	0.049 (0.007)	1.765 (0.858)
Chevron Corp.	0.021 (0.005)	0.029 (0.006)	0.031 (0.007)	0.736 (0.284)
Coca-Cola Co.	0.057 (0.018)	0.012 (0.001)	0.034 (0.004)	1.184 (0.352)
E.I. DuPont & Co.	0.113 (0.025)	0.013 (0.002)	0.051 (0.006)	1.690 (0.918)
Exxon Mobil Corp.	0.053 (0.021)	0.008 (0.002)	0.025 (0.006)	0.567 (0.321)
General Electric Co.	0.094 (0.003)	0.013 (0.004)	0.041 (0.001)	0.802 (0.331)
Hewlett-Packard Co.	0.055 (0.039)	0.033 (0.005)	0.053 (0.013)	1.937 (0.660)
Home Depot Inc.	0.096 (0.010)	0.012 (0.002)	0.040 (0.004)	1.633 (0.570)
IBM Corp.	0.077 (0.023)	0.016 (0.004)	0.047 (0.009)	1.782 (0.727)
Johnson & Johnson	0.058 (0.016)	0.005 (0.001)	0.021 (0.004)	0.670 (0.310)
JPMorgan Chase & Co.	0.082 (0.013)	0.017 (0.003)	0.051 (0.008)	0.927 (0.501)
Kraft Foods Inc. Cl A	0.049 (0.014)	0.034 (0.004)	0.051 (0.006)	1.992 (0.676)
McDonald's Corp.	0.042 (0.019)	0.035 (0.003)	0.050 (0.011)	1.707 (0.727)
Merck & Co. Inc.	0.064 (0.025)	0.018 (0.004)	0.046 (0.013)	1.709 (0.965)
Pfizer Inc.	0.043 (0.018)	0.012 (0.001)	0.028 (0.005)	1.134 (0.375)
Procter & Gamble Co.	0.067 (0.014)	0.014 (0.003)	0.039 (0.006)	0.966 (0.468)
Travelers Cos. Inc.	0.076 (0.008)	0.024 (0.004)	0.058 (0.007)	1.382 (0.671)
United Technologies	0.050 (0.016)	0.024 (0.002)	0.045 (0.006)	1.654 (0.587)
Verizon Communications	0.056 (0.013)	0.041 (0.017)	0.021 (0.006)	3.391 (1.764)
Wal-Mart Stores Inc.	0.066 (0.020)	0.012 (0.002)	0.037 (0.007)	1.374 (0.574)
Walt Disney Co.	0.037 (0.020)	0.050 (0.008)	0.055 (0.012)	2.554 (0.736)
Average	0.068 (0.018)	0.021 (0.004)	0.041 (0.007)	1.570 (0.661)

This table summarizes the mean of the estimated parameters of the one-factor CIR model $\left(\kappa^{\lambda}, \theta^{\lambda}, \sigma^{\lambda}\right)$ for the default intensity λ_0 between January 2005 and June 2007. These parameters are estimated for 27 component companies of the DJIA using CDS spreads with maturities of $t = 1, 3, 5, 7$ and 10 years. The numbers in parentheses are the standard deviation. The mean of the root mean square errors (RMSE) of the estimated CDS spreads for the same period is also reported. The RMSE and its standard deviation are presented in basis points.

Table 6. Estimated CIR parameters: CDS spreads, July 2007-June 2010

Company Name	**July 2007 - June 2010**			
	κ^λ	μ^λ	σ^λ	**RMSE (bps)**
3M Co.	0.228 (0.078)	0.015 (0.007)	0.068 (0.022)	1.955 (1.178)
Alcoa Inc.	0.139 (0.131)	0.099 (0.052)	0.133 (0.032)	9.022 (8.031)
American Express Co.	0.367 (0.208)	0.023 (0.009)	0.098 (0.038)	4.683 (3.515)
AT&T Inc.	0.081 (0.024)	0.029 (0.011)	0.030 (0.016)	2.020 (0.908)
Bank of America Corp.	0.263 (0.107)	0.023 (0.009)	0.093 (0.025)	7.707 (5.530)
Boeing Co.	0.345 (0.216)	0.025 (0.009)	0.101 (0.047)	3.283 (2.692)
Caterpillar Inc.	0.258 (0.201)	0.025 (0.011)	0.082 (0.046)	3.067 (2.768)
Chevron Corp.	0.196 (0.138)	0.022 (0.009)	0.070 (0.028)	1.730 (1.133)
Coca-Cola Co.	0.198 (0.130)	0.019 (0.008)	0.068 (0.021)	1.871 (0.847)
E.I. DuPont & Co.	0.342 (0.248)	0.019 (0.006)	0.095 (0.037)	3.482 (3.052)
Exxon Mobil Corp.	0.218 (0.121)	0.013 (0.006)	0.062 (0.023)	1.467 (0.690)
General Electric Co.	0.130 (0.107)	0.087 (0.072)	0.119 (0.043)	8.993 (7.436)
Hewlett-Packard Co.	0.198 (0.121)	0.020 (0.010)	0.070 (0.016)	2.484 (1.396)
Home Depot Inc.	0.356 (0.160)	0.030 (0.013)	0.123 (0.031)	6.605 (4.553)
IBM Corp.	0.244 (0.116)	0.016 (0.006)	0.077 (0.017)	2.368 (1.244)
Johnson & Johnson	0.094 (0.021)	0.015 (0.005)	0.045 (0.012)	1.707 (0.931)
JPMorgan Chase & Co.	0.344 (0.141)	0.018 (0.005)	0.104 (0.032)	4.503 (2.896)
Kraft Foods Inc. Cl A	0.241 (0.114)	0.025 (0.008)	0.088 (0.022)	2.956 (1.933)
McDonald's Corp.	0.119 (0.059)	0.018 (0.008)	0.058 (0.015)	2.191 (1.122)
Merck & Co. Inc.	0.121 (0.046)	0.015 (0.003)	0.057 (0.014)	2.141 (3.021)
Pfizer Inc.	0.232 (0.112)	0.016 (0.004)	0.074 (0.023)	1.708 (0.827)
Procter & Gamble Co.	0.279 (0.093)	0.016 (0.006)	0.084 (0.027)	1.958 (0.848)
Travelers Cos. Inc.	0.268 (0.081)	0.019 (0.004)	0.093 (0.017)	2.882 (2.740)
United Technologies	0.211 (0.121)	0.020 (0.007)	0.080 (0.027)	1.997 (1.050)
Verizon Communications	0.307 (0.149)	0.023 (0.008)	0.074 (0.036)	3.678 (2.292)
Wal-Mart Stores Inc.	0.208 (0.102)	0.015 (0.003)	0.072 (0.022)	2.088 (1.234)
Walt Disney Co.	0.170 (0.126)	0.028 (0.016)	0.074 (0.020)	2.891 (1.652)
Average	0.228 (0.121)	0.026 (0.012)	0.081 (0.026)	3.387 (2.427)

This table summarizes the mean of the estimated parameters of the one-factor CIR model $\left(\kappa^\lambda, \theta^\lambda, \sigma^\lambda\right)$ for the default intensity λ_0 from July 2007 to June 2010. These parameters are estimated for 27 component companies of the DJIA using CDS spreads with maturities of $t = 1, 3, 5, 7$ and 10 years. The numbers in parentheses are the standard deviation. The mean of the root mean square errors (RMSE) of the estimated CDS spreads for the same period is also reported. The RMSE and its standard deviation are presented in basis points.

Figure 1. Performance of the Nonlinear Filter on Simulated CDS Spreads

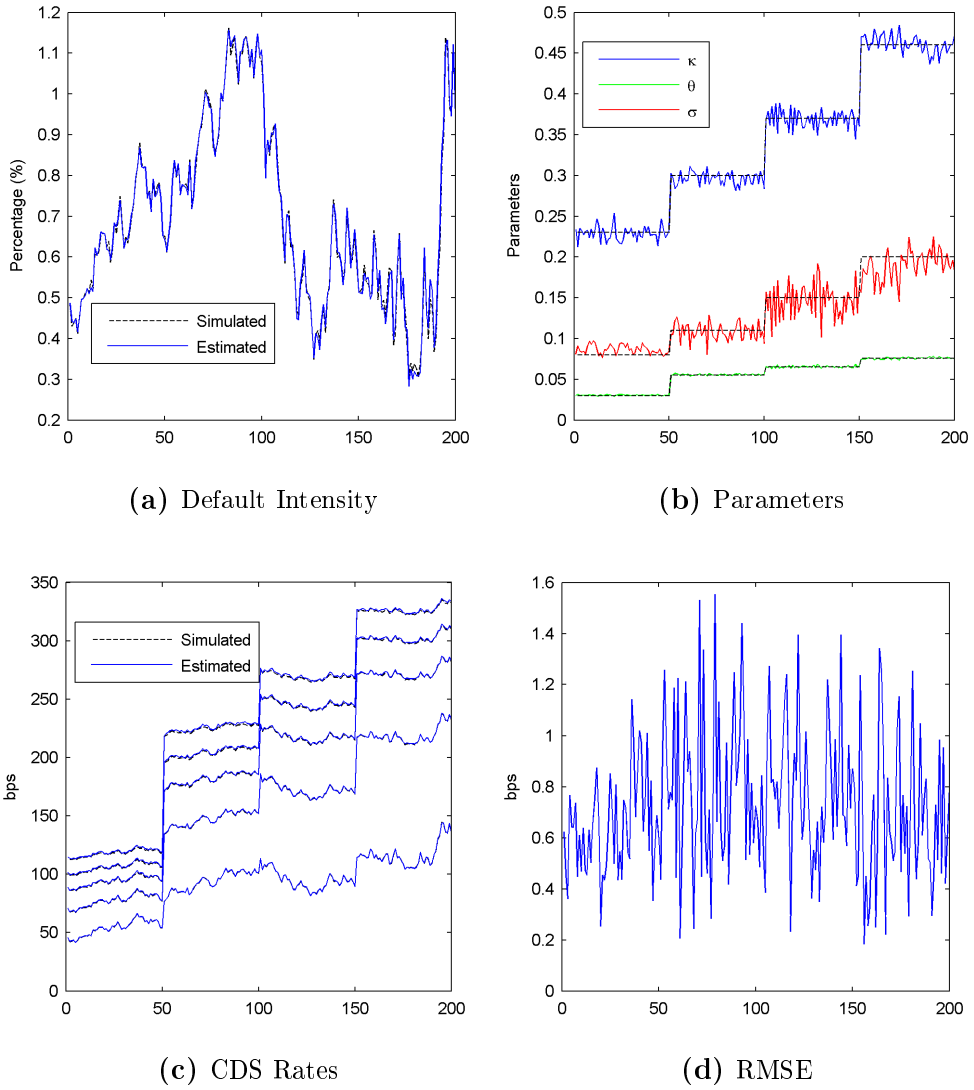

(a) Default Intensity **(b)** Parameters

(c) CDS Rates **(d)** RMSE

This figure shows the performance of the nonlinear filter on simulated CDS spreads data. Panel A plots the simulated and estimated values of the default intensity λ_s. Panel B compares the values of the parameters of the one-factor CIR model $\psi_s^\lambda = [\kappa^\lambda, \theta^\lambda, \sigma^\lambda]$ used in the simulation and those estimated with the filter. Panel C shows the simulated and estimated CDS spreads for maturities $t = 1, 3, 5, 7$ and 10 years. In Panels A and C, the simulated values are plotted in black while estimated values are in blue. Panel D presents the RMSE of the estimated CDS spreads. The simulated values are assumed as benchmark.

Figure 2. Estimation of the short interest rate and CIR model parameters

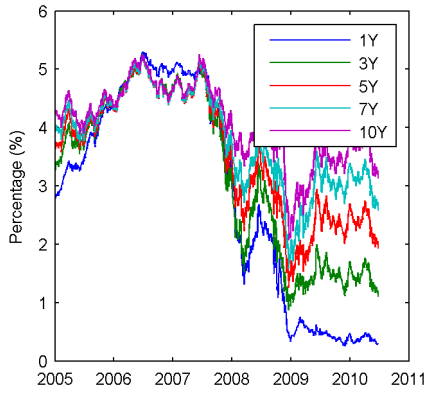

(a) Treasury Constant Maturity Rates

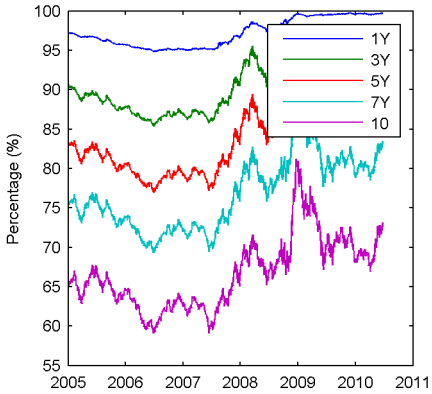

(b) Zero-Coupon Bond Prices

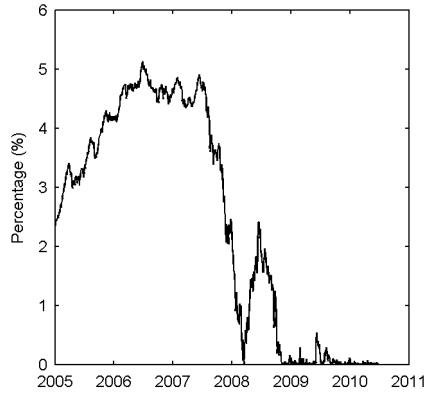

(c) Estimated Short Interest Rate r_0

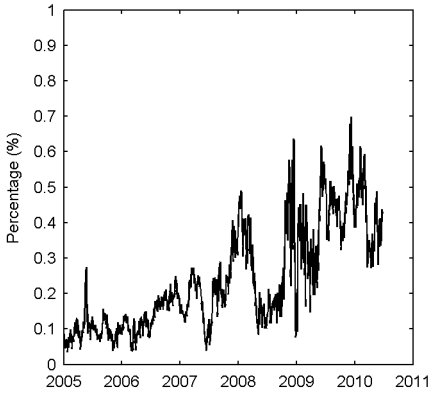

(d) Estimated Error

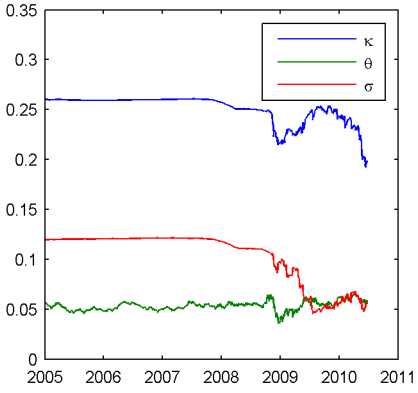

(e) Estimated Parameters

This figure shows the performance of the nonlinear filter in inferring the short interest rate r_0 from zero-coupon bond prices. Panel **(a)** shows the US treasury constant maturity bond rates. Following Chen et al. (2008b) , these rates are used to compute the zero-coupon bond prices in Panel **(b)**. The maturities considered are $t = 1, 3, 5, 7$ and 10 years. Panels **(c)** and **(e)** show the evolution of the estimated short interest rate r_0 and the one-factor CIR parameters $\boldsymbol{\psi}_s^r = [\kappa_s^r, \theta_s^r, \sigma_s^r]$. Panel **(d)** presents the root mean square errors (RMSE) of the estimated zero-coupon bond prices. The values of Panel **(b)** are taken as benchmark.

Figure 3. Estimated default intensity by industry

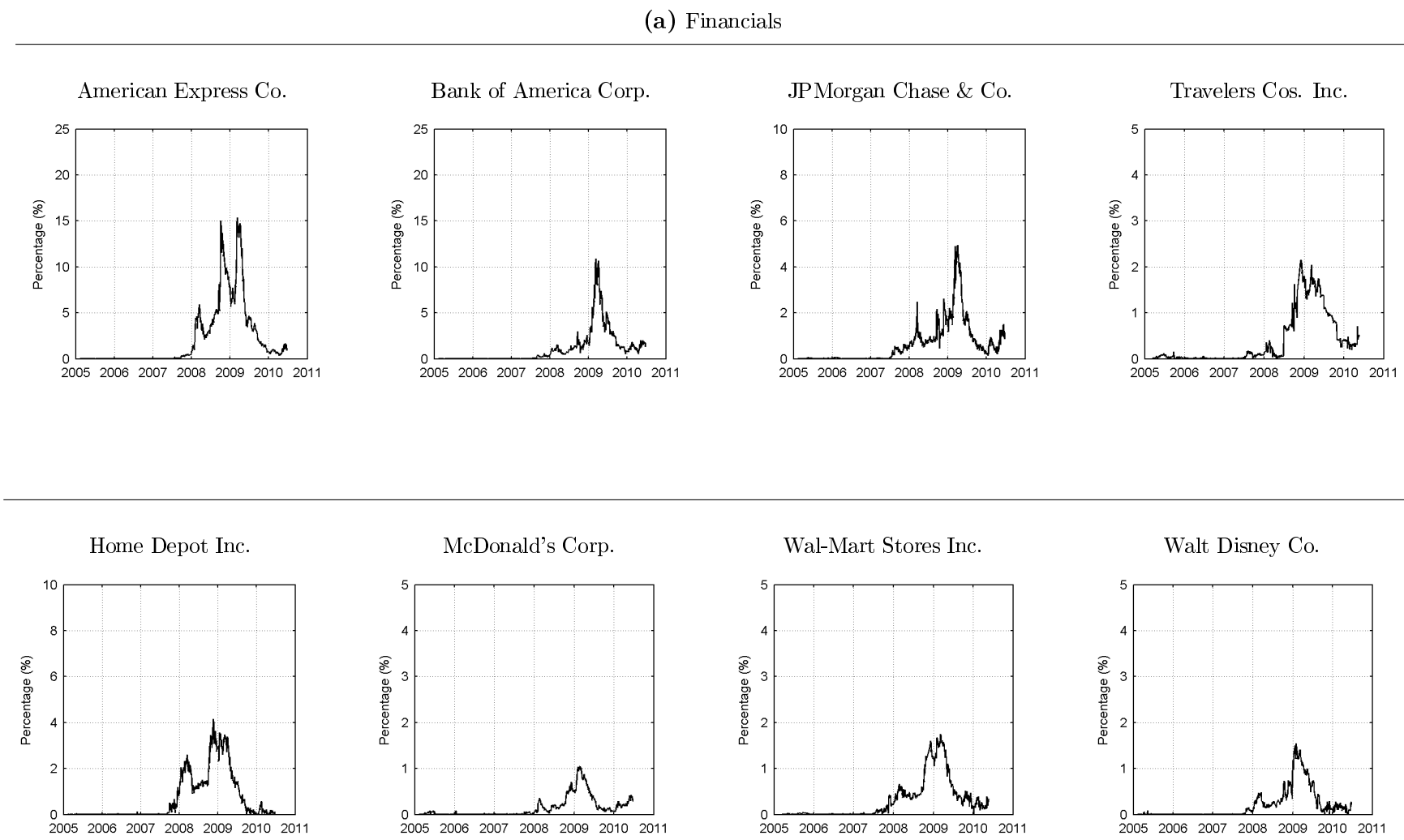

This figure shows the evolution of the estimated default intensity λ_0 for 27 component companies of the DJIA between June 2005 and June 2010. The default intensity λ_0 is inferred from CDS spreads with maturities $t = 1, 3, 5, 7$ and 10 years using the nonlinear filter. Panel **(a)** shows the companies in the financial industry while Panel **(b)** presents the companies in the sector of consumer services. The values are in percentages.

Figure 3. Estimated Default Intensity by Industry (cont'd)

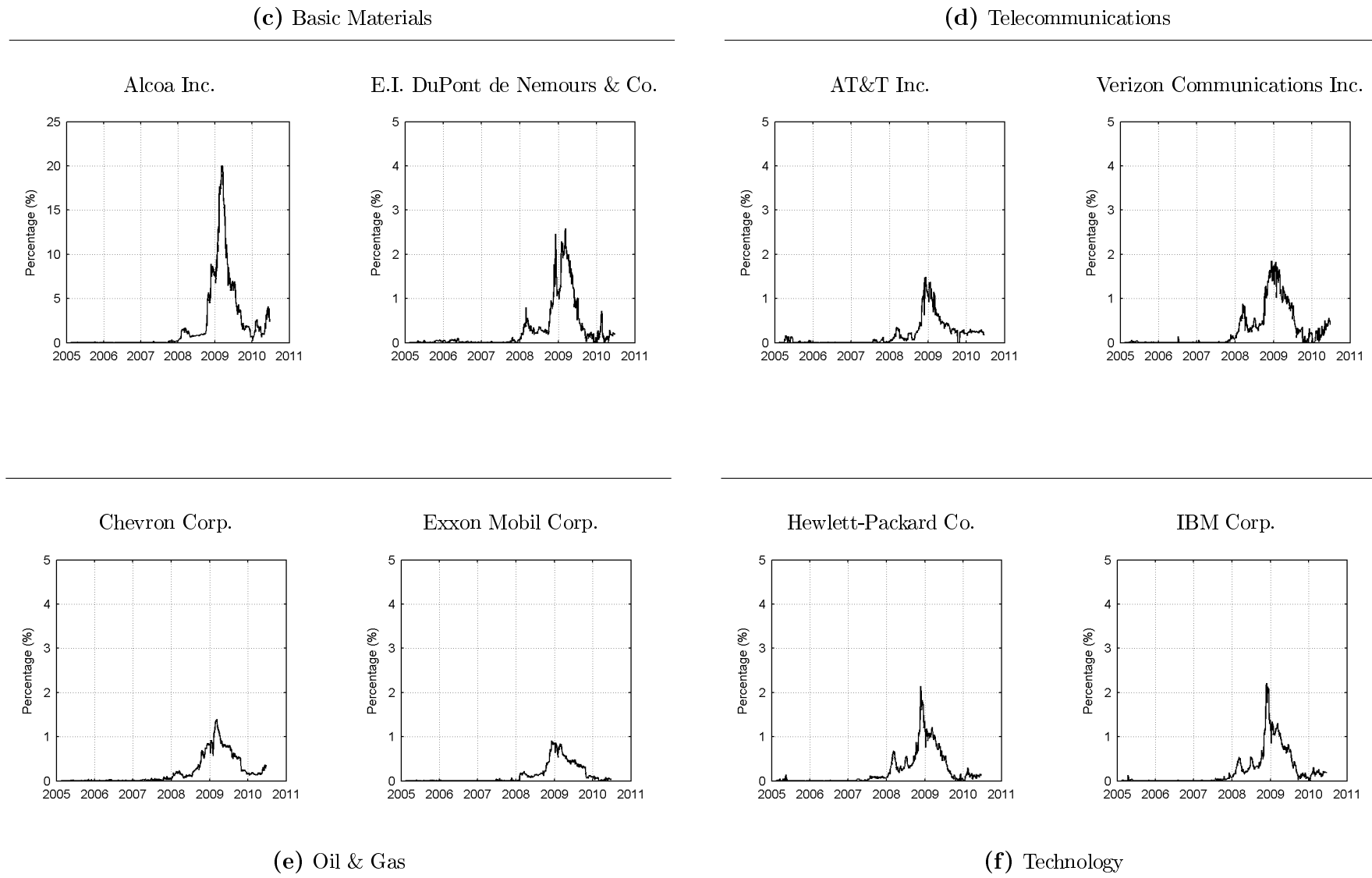

This figure shows the evolution of the estimated default intensity λ_0 for 27 component companies of the DJIA between June 2005 and June 2010. The default intensity λ_0 is inferred from CDS spreads with maturities $t = 1, 3, 5, 7$ and 10 years using the nonlinear filter. Panel **(c)**, **(d)**, **(e)** and **(f)** show the companies in the sectors of basic materials, telecommunications, oil & gas and technology, respectively. The values are in percentages.

Figure 3. Estimated Default Intensity by Industry (cont'd)

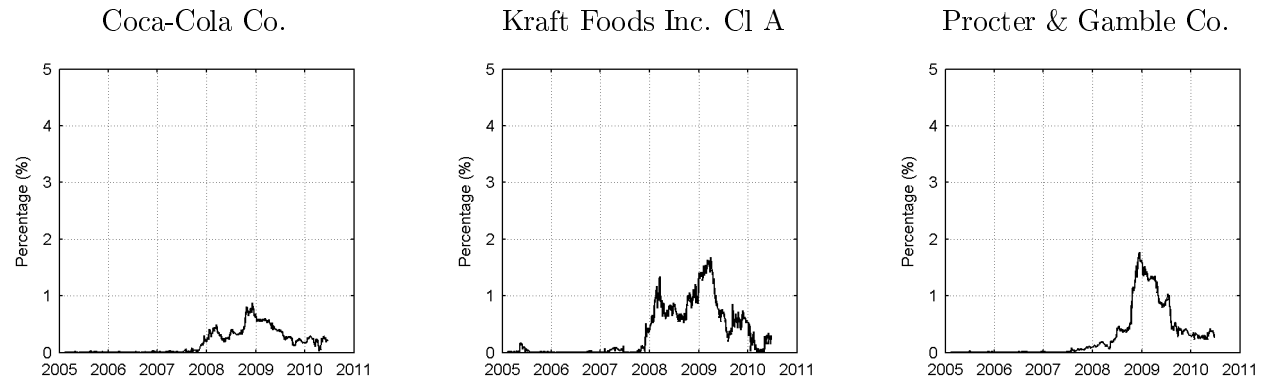

(g) Consumer Goods

(h) Health Care

This figure shows the evolution of the estimated default intensity λ_0 for 27 component companies of the DJIA between June 2005 and June 2010. The default intensity λ_0 is inferred from CDS spreads with maturities $t = 1, 3, 5, 7$ and 10 years using the nonlinear filter. Panel **(g)** shows the companies clustered in the sector of consumer goods. Panel **(h)** presents the companies in the industry of health care. The values are in percentages.

Figure 3. Estimated Default Intensity by Industry (cont'd)

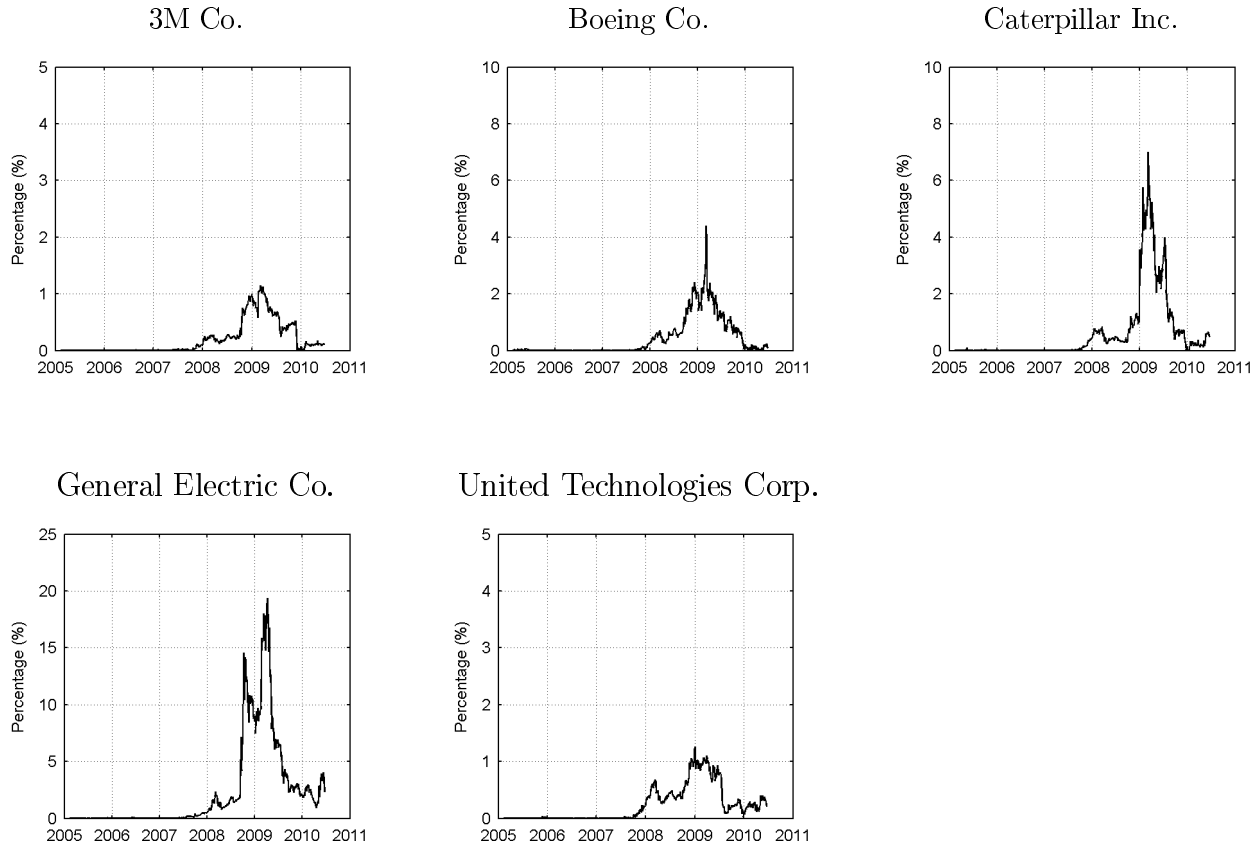

(i) Industrials

This figure shows the evolution of the estimated default intensity λ_0 for 27 component companies of the DJIA between June 2005 and June 2010. The default intensity λ_0 is inferred from CDS spreads with maturities $t = 1, 3, 5, 7$ and 10 years using the nonlinear filter. Panel **(i)** shows the companies clustered in the industrial sector. The values are in percentages.